ABSTRACT

SICO, KATHLEEN BEETLE. PMU Data Analysis and Short-term Voltage Stability Assessment. (Under the direction of Dr. Aranya Chakrabortty.)

The number of Phasor Measurement Units (PMUs), also called synchrophasors, located across the country has been growing at an astronomical rate. When coupled with existing construction and maintenance work these devices are inexpensive to implement and provide valuable data. Now that the PMU infrastructure is in place, there have been many efforts to optimize the use of this data. Given the amount of data, between 30 to 120 samples per second from each PMU over several measurements, there is a need to develop innovative ways to process the data and create useful applications for system planners, operators and protection engineers. Duke Energy has installed 125 PMUs across a portion of its service territory and provided this data for research by a team with members from Duke Energy, SAS and North Carolina State University (NCSU). This team is tasked with working through data acquisition, examining data quality, baselining and ultimately exploring possible synchrophasor based applications. This thesis covers the work completed at NCSU towards this project. First, PMU based applications that have been covered in recent literature are explored. Next baselining results are reviewed including some baselining around events looking at ranges of voltage magnitude, frequency and voltage phase angle difference as well as dynamic baselineing, evaluating the slow modes or frequencies of the system. After the baselining results the application of PMU data in voltage stability assessment is more thoroughly reviewed. Since short-term voltage instability can lead to collapse in under five seconds it is important to evaluate the predictive nature of these methods which would allow time for corrective action by system operators. Two methods are tested and compared, the Lyapunov Exponent (LE) and the decision tree.

PMU Data Analysis and Short-term Voltage Stability Assessment

by
Kathleen Beetle Sico

A thesis submitted to the Graduate Faculty of
North Carolina State University
in partial fulfillment of the
requirements for the Degree of
Master of Science

Electrical Engineering

Raleigh, North Carolina

2014

APPROVED BY:

Dr. David Lubkeman	Dr. Ning Lu

Dr. Aranya Chakrabortty
Chair of Advisory Committee

DEDICATION

I would like to dedicate this thesis to my husband Vince Sico. He is the one who encouraged me to return to school and has provided me with love and support throughout my journey. I couldn't have imagined accomplishing what I have with out him by my side.

BIOGRAPHY

Kathleen Beetle Sico was born in Los Gatos, California on the 5th of May 1975. She completed high school at Walter Hines Page High School in Greensboro, North Carolina in the Spring of 1994. She went on to pursue a Bachelors of Arts degree in Psychology from the University of California Santa Cruz graduating in 1998. In 2008 she decided to return to school to pursue a Bachelors of Science degree in Electrical Engineering which turned into the pursuit of a Masters degree with a focus on power systems at North Carolina State University (NCSU).

In order to get experience and affirm her new career decision Kathleen Sico decided to enroll in the Cooperative Education Program with Duke Energy starting the Fall of 2011. During her rotations she worked with Substation Electrical and Control Design, Power Delivery Engineering University and Protection and Controls Engineering. Starting in the Fall of 2013 she has been working on the PMU data analysis project, that is the topic of this thesis, with Duke Energy, SAS Institute and Dr. Aranya Chakrabortty at NCSU. During the Summer of 2014 she worked on a separate project at Duke Energy's Energy Control Center (ECC) looking at angular (transient) stability of generating units for a delayed clearing fault. She has excepted an offer to work as an Engineer I at the ECC starting in January 2015.

Apart from her school and career, Kathleen has a loving husband that she has been married to since October 2009. Their life together has been enriched by the birth of their first daughter Violet Sico in December of 2013. She is looking forward to her new career and being able spend more time doing fun family activities.

ACKNOWLEDGEMENTS

There are several people I would like to acknowledge for their support and/or contributions to this project. First I would like to thank my advisor Dr. Aranya Chakrabortty and my supervisor at Duke Energy Mr. Tim Bradberry for giving me the opportunity to be involved in this cutting edge research. I am lucky to have had the chance to work with Dr. Chakrabortty, who is at the forefront of research using WAMS technology. He is also one of the best instructors that I have had, he enjoys teaching as well as research and I have learned a lot from his courses. Tim Bradberry is a very supportive supervisor who has been flexible and understanding of the balance between work and life which is important for a new mother. He has provided a lot of useful feedback and I hope he has found the results of this research effort promising for the incorporation of PMU data at Duke Energy. I would also like to thank Dr. David Lubkeman and Dr. Ning Lu for being part of my graduate committee. Dr. David Lubkeman is an incredible instructor and has, what seems to be an infinite amount of knowledge, regarding SCADA systems and communication. Although I have not had the pleasure of taking a course with Dr. Ning Lu she has background in the research regarding the analysis and modeling of load behaviors which is an important part of voltage stability assessment.

John O'Connor from Duke Energy has been an integral part of the team providing invaluable information regarding real system phenomena and specific information regarding Duke Energy. He is a principle engineer with system planning and is an expert in dynamic stability. John is not only my colleague but a mentor, friend, advocate and source of inspiration. From his help in teaching me the basics of PSSE and dynamic simulations to the theory behind the results I was able to build confidence in my findings. I am lucky to have John as part of my team and can only hope to accel as he has in my future career.

I would like to acknowledge the other members of our research team from SAS. Greg Link is responsible for organizing the team at SAS for this research effort, has a background experience in the utility business and from this has provided many ideas regarding the possible uses of the PMU data. Brad Klenz is an expert with the analysis of big data from various sources and has provided the team with some insight to big data and statistics which at times would be overlooked by people with utility experience. His knowledge and creativity have been one of the biggest assets to our team. Brad and I worked together closely on the decision tree portion of this thesis and I learned a lot from him regarding the creation and results of this tool. I would like to acknowledge Glenn Lampley for his input to this research effort. With prior utility experience he was able to share ideas, such as detection of equipment failure as a possible use of the PMU data. Last but not least I would like to acknowledge Dr. Arnie DeCastro from SAS. He was able to understand and contribute to some of the higher level concepts discussed and

evaluated during this research effort.

I would like to thank everyone who gave me support from Duke Energy. Megan Vutsinas was my contact for all of this data analysis and any information we needed regarding the PMUs on the Duke Energy System. In addition Megan also provided me with resource materials from current efforts in the analysis and use of PMU data. Brian Moss provided me with the resources that we needed to complete the voltage stability simulations. Evan Phillips and Stephen Shuford provided support with accessing the PMU data as well as using the EPG tools RTDMS and PGDA. Linwood Ross verified the PSSE channel file buses and lines matched the location of the PMUs in the voltage sensitive region. Doug Steinback and Scott Nyberg helped me obtain and understand the equivalent impedance of the transmission corridor used for the PV analysis. In addition, I would like to thank Sammy Roberts, Daniel Stephens and everybody at the ECC. The wealth of knowledge obtained through my internship at the ECC has helped me better assess the usefulness of the PMU data in operations.

I would like to thank the FREEDM Center for providing the space and resources for this research effort. Karen Autrey organized our monthly meetings and assisted with technical issues encountered along the way. Dr. Chakrabortty's research team provided inspiration and support during my research as well as providing me feedback for my oral examination. In particular I would like to thank Abhishek Jain who taught me how to use Latex, saving me countless hours of formatting, and provided encouragement, support and honest feedback.

Finally, I would like to thank my family who has supported me in all my endeavors and has always encouraged my efforts. My husband and daughter have put up with my stress and limited amount of time and attention. My husbands parents who have made many trips to our house to watch my daughter and who have helped with many other aspects of day to day life. I couldn't have asked for better in-laws, they have been a blessing to have as family. My brother and sister-n-law have also contributed many hours and trips to my house to watch my daughter allowing me the extra time I needed to accomplish what I have.

TABLE OF CONTENTS

LIST OF TABLES

LIST OF FIGURES

Chapter 1

Introduction

The number of Phasor Measurement Units (PMUs) located across the country has been growing at an astronomical rate as shown in figure 1.1 [2]. Many of these have been installed under smart grid initiatives of the US Department of Energy (DOE)[3]. When coupled with existing construction and maintenance work, these devices are inexpensive to implement and provide valuable data.

The PMU, also known as a synchrophasor was introduced in the mid 1980's and was first developed at Virginia Tech. Early funding for its development came from the US DOE, the US Electric Power Institute (EPI) and the US National Science Foundation(NSF). The first installations were in the Bonneville Power Administration (BPA), American Electric Power (AEP) and New York Power Authority (NYPA) service areas. The PMU combines some of the technology that was introduced in the Symmetrical Component Distance Relay (SCDR) of the late 1970's with the synchronized GPS clock signal. The GPS clock can achieve accuracy of 1 μs which correlates to an angle of 0.021 degrees. The SCDR used a recursive algorithm to calculate the symmetrical components of voltage and current using the Discrete Fourier Transform (DFT) [4].

Historically the most accurate frequency measurement was at generating stations and reflected the speed of the rotor which is directly related to the frequency of the generator voltage (i.e. Watt-Type fly-ball governor of steam turbines). Another method for measuring frequency is to calculate it from the zero crossings of the voltage. The phasors calculated by the PMU reflect the fundamental frequency component of the voltages and is not affected by harmonics. This technology also extends the frequency measurement to system buses. Power system frequency measurements are for estimating the rotor speed of the systems generators [5].

The ability for this device to accurately measure phase angle with a synchronized GPS timestamp across large geographical areas makes it ideal for wide area measurements. Synchrophasor technology is often referred to as Wide Area Measurement System (WAMS) technology [3]. Since

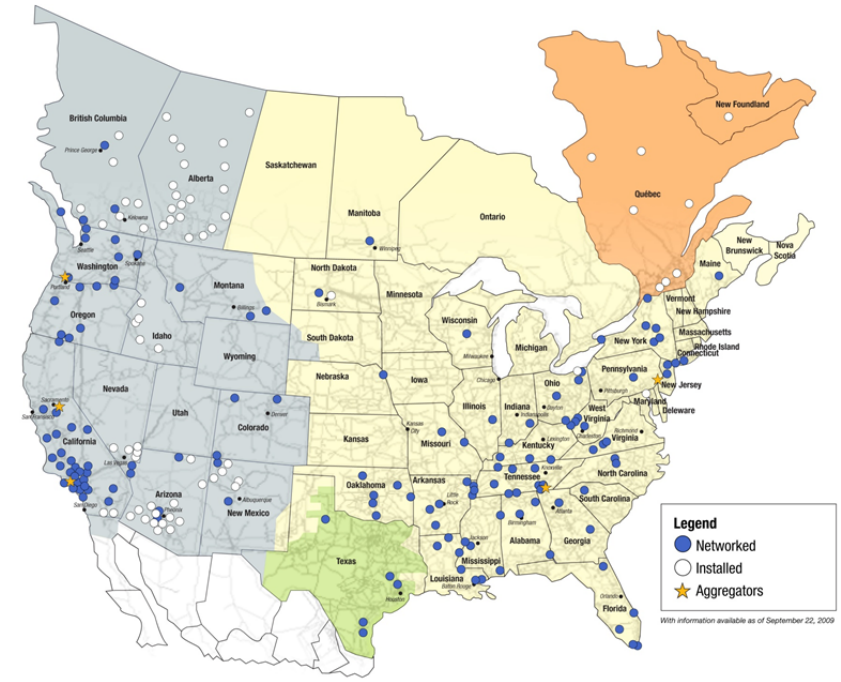

(a)

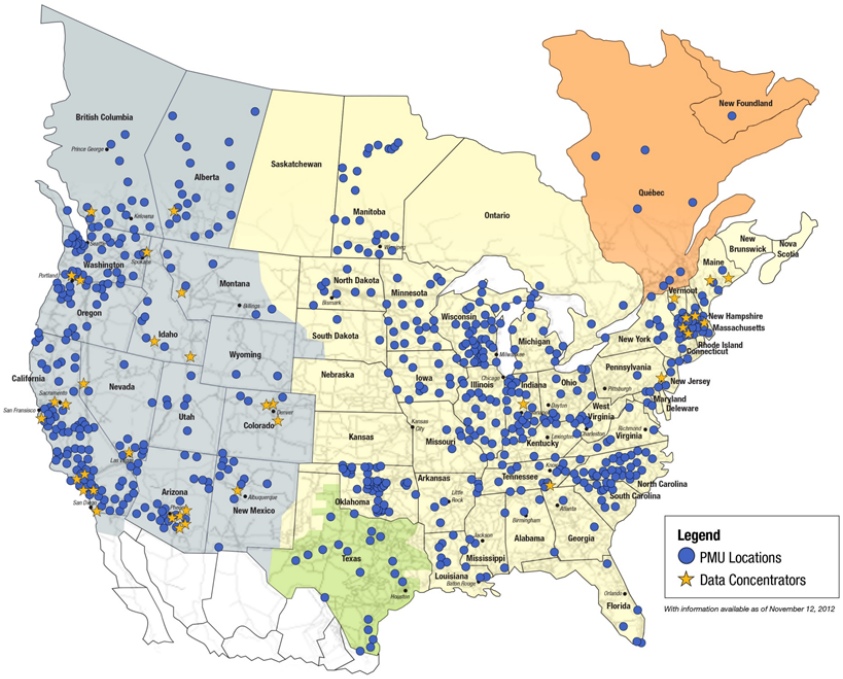

(b)

Figure 1.1: PMUs in the United States (a) 2009 [2] (b) 2012 [2]

real power flows from large phase angle to small phase angle these measurements can be used to indicate how the power is flowing across a system. Much of the research that has been conducted on WAMS has focused on using the measurements for monitoring and situational awareness of large power systems across a large geographical area [3]. Most PMU placement methods focus on power system observability [6].

1.1 Synchronized Phasor Measurements

Synchronized phasor measurements provide positive sequence voltage and current measurements synchronized within 1 μs and local frequency measurements. They can also measure harmonics , negative sequence, zero sequence and phase voltages [5]. A phasor contains information about the magnitude and angle of a sinusoidal waveform. The angle is the deviation from a referenced time or angle as shown in Figure 1.2 [2]. Given the following sinusoidal function

$$f(t) = V\cos(\omega t + \delta) \tag{1.1}$$

Using Euler's formula we can rewrite (1.1).

$$f(t) = V * \frac{e^{j(\omega t+\delta)} + e^{-j(\omega t+\delta)}}{2} \tag{1.2}$$

By extracting the real portion of (1.2) we have

$$f(t) = Re\{Ve^{j(\omega t+\delta)}\} \tag{1.3}$$

Since we know the frequency we can eliminate this term in the shorthand notation of the phasor expression and write

$$f(t) = Ve^{j\delta} = V\angle\delta \tag{1.4}$$

Phasor representation is only possible for a pure sinusoid. All signals from the power system will have components of multiple frequencies. In order obtain a phasor measurement a single frequency needs to be isolated. Ultimately the signal can be expressed as a sum of sinusoids, or a fourier series, and from this the pure sinusoid at the fundamental frequency can extracted. The Discrete Fourier Transform (DFT)is the process used with sampled data. This process is explained in detail in [5].

These voltage measurements are taken from the bus potential transformer (PT) or capacitance coupled voltage transformer (CCVT) and the current measurements are taken from the line current transformer (CT) and possibly another shared breaker CT depending on the bus configuration. In the example of a breaker and a half scheme shown in the Figure 1.3 the current

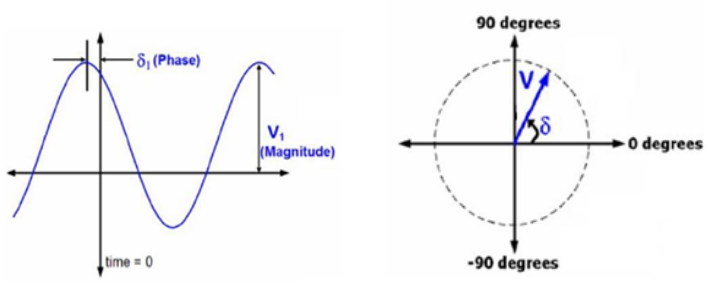

(a) **(b)**

Figure 1.2: (a) Sinusoidal Waveform [2] (b) Phasor Representation [2]

measurement would be the addition of the current measured at the line breaker CT and the current measured at the tie breaker CT. The ratios of these transformers are entered into the settings of the phasor measurement unit so that the actual voltage and current at the bus and on the line are displayed.

1.2 Motivation of the Study

Since the concept, development, installation and implementation of these devices there are a few things to consider. The amount of data that is measured and sent to a Phasor Data Concentrator (PDC) at 30 to 120 samples per second from each PMU is far too much for the operator to make any sense of on a real-time basis. Tools must be created to process the data and provide useful information to system planners, operators and protection engineers. Ultimately the million dollar question is..."Now that we have all this data, how can we use it to improve our situational intelligence" [2]?

Duke Energy has installed 125 PMUs across a portion of its territory and has provided this data to a team consisting of members from Duke Energy, SAS and NCSU for research. This team is tasked with working through data acquisition, examining data quality and data analysis including baselining and exploring synchrophasor based applications for system planners, operators and protection engineers. With help from our collaborators from SAS institute we completed the data acquisition, data quality and baselining in the Fall of 2013. In the early part of 2014 we started to explore possible applications for the PMU data.

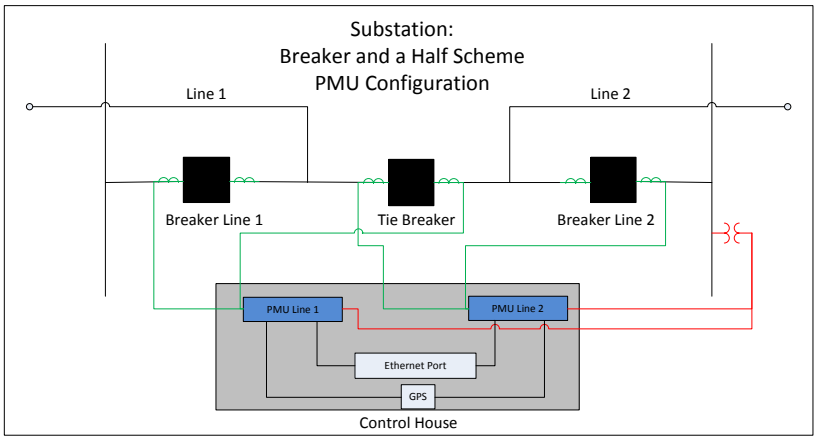

Figure 1.3: PMU Configuration

1.3 Literature Review

There is a limited amount of literature surrounding baselining of PMU data. The importance of baselining PMU data is that it can reveal different relationships and insights given the higher time resolution according to [7]. This article suggests that we need a longer history of PMU data to enable more sophisticated baselining techniques. In [8] offline studies of EMS state-estimator data and stability simulations coupled with data mining techniques are used in the baselining of phase angle versus power transfer limits to provide synchrophasor-based situational awareness.

Initial research on the possible applications of syncrophasors was conducted by Virgina Tech and Cornell University through funding from BPA, AEP and NYPA[4]. There are several applications that are a topic of research in which few have been implemented. Of these applications most of them focus on monitoring and situational awareness with a few applications in the control arena [3]. Possible synchrophasor applications reviewed are listed below.

- Phasor state estimation
- Dynamic model validation
- Dynamic stability assessment and instability detection
- Visualization of dynamic attributes
- System identification

- Constructing simplified inter-area models
- Protection systems with phasor inputs
- Wide Area control with phasor feedback

There are many papers that discuss using PMU measurements either in combination with SCADA measurements or stand alone for the state estimator. When in combination, the PMU measurements are seen as normal measurements and applied as part of the nonlinear state estimation. When only PMU measurements are used and the system is fully observable, linear state estimation can be accomplished [9].

The state estimator was developed as a better algorithm for more accurately estimating the state of the system than the traditional load flow. This algorithm takes a large number of imprecise measurements as inputs and estimates the real and reactive power flowing on the lines as well as the voltage magnitudes and angles at all the buses. Since the bus voltage magnitudes and angles determine the system power flows and power injections they are considered the state of the system [5]. Therefore, the PMUs are actually able to measure the states of the system without estimation at the buses where they are located. The voltage magnitude and angle at all of the neighboring buses can be calculated using the current magnitude and angle measurements and information on the impedance of the line.

Incorporating PMU measurements with existing SCADA measurements in state estimation is proposed in [10]. In [11] it was found that adding measurements from PMUs in sufficient numbers increases the efficiency and precision of state estimation. When using a topological algorithm for state estimation, [12] shows that PMU based algorithms are computationally more simple, systematic and efficient than conventional ones. There are also many papers that explore methods in determining optimal PMU locations to make the measurement model observable such as shown in [13].

PMU measurements can be used to validate the dynamic model of a complete system, individual generators, aggregate dynamic loads and Flexible AC Transmission System (FACTS) devices. Since the sampling rate is high enough to observe post event oscillations this can be compared to results of dynamic simulations using tools such as Power System Simulator for Engineering (PSSE). In [14] post event analysis using PMU measurements were able to verify system dynamic simulation studies in the Electric Reliability Council of Texas (ERCOT) and enable them to verify dynamic models of conventional and wind generators. Real-time dynamic modeling, validation and tuning of a synchronous generator was accomplished using Real Time Digital Simulator (RTDS), PMU measurements and IEC 61850 communication protocol [15]. There has also been work on model validation of FACTS devices, particularly a Static Var Compensator (SVC) and a Static Synchronous Compensator (STATCOM), also known as a

Static Synchronous Condensor [16].

The area that has received the most attention as far as application development is concerned is dynamic stability assessment and detection. There are three main types of dynamic stability. First there is small-signal stability which focuses on the slow dynamic inter-area oscillations remaining bounded. Second there is transient stability also termed 'first swing' stability which focuses on the initial swing of a synchronous generators' rotor angle after a disturbance. Finally there is voltage stability which is a more localized phenomenon that occurs at load centers in which the voltage depresses below an acceptable level for an extended period of time.

There have been several papers on using PMU data to assess and detect small-signal stability which is important for systems with clustered generation and load pockets separated by long transmission lines. Most of this research has been based on the fact that power system mode shapes can determine the participation of different dynamic components in the low-frequency inter-area oscillations. These modes are calculated from a linearized dynamic model. Since large scale accurate dynamic power system models are difficult to obtain, measurement based methods have been receiving a lot of attention since they can be created in real-time with PMU data. Finding these mode shapes through PMU measurements have the advantage of real-time applications for small-signal stability [17] and the damping of inter-area oscillations.

In [17] a least squares method is used to estimate modes through an auto-regressive exogenous model. In [18] a recursive method of Prony analysis is used to detect ringdown data using phasor measurements. Ringdown data is the data that results after a large disturbance in which observable oscillations are present. This data can be used to detect the slow inter-area modes of a system and therefore assist with small-signal stability [18]. A method using PMU data to monitor the dynamic status of power transfer paths with adapted energy function analysis is proposed in [19]. This energy can be decomposed into a swing and slow quasi-steady-state components which can be used to monitor damping and transfer path synchronizing stability respectively. This method is demonstrated on real PMU data from the WECC system which recorded an event causing 0.578 Hz oscillations along a transfer path 600 miles long from a median size group of machines supplying power to a remote load center which lasted a total of 5 minutes. In [20] an automated real-time oscillation monitoring system for small-signal instability detection without need for human intervention during analysis is proposed. This is realized using the classical multi-input Prony algorithm, the matrix Pencil algorithm and the Hankel total least square method. This monitoring tool will issue operator alerts and control triggers when the damping level of these mode oscillations reach predetermined thresholds. An added benefit to assessing small-signal stability is the possibility of adding control in the form of inter-area oscillation damping. A method for accomplishing this is proposed in [21] and consists of three steps. First the PMU data is used to identify second order aggregate models for the oscillation clusters of the system allowing for a reduced model of the system to be created.

Second a desired closed loop transient response is achieved between each cluster pair of the reduced model using state-feedback controllers. Finally an aggregate distributed control design is tuned to realistic generator controls until the response of the real full order system matches the desired response of the reduced order system.

Normally, transient stability is assessed by looking at the post disturbance values of generator rotor angles. The assessment of transient stability was usually based on offline simulations using the system model with assumed system conditions and contingencies based on intelligent decisions made by subject matter experts with knowledge of system vulnerabilities. Since the implementation of WAMS technology there has been research on fast detection of transient stability using PMU data. Some algorithms have used voltage phase angle and frequency measurements to determine transient stability. One of these algorithms uses the synchronized phase angle to determine if any angle deviation in a particular area start to move away from a center of inertia reference. Another method approximates the potential and kinetic energy of generators using voltage phase angle and frequency measurements. An additional algorithm quantifies the stability threshold along system trajectories [22]. In [23] a method using PMU data and artificial neural networks (ANN) for transient stability prediction in real-time is proposed. This paper further proposes a transient instability mitigating control scheme that involves intentional islanding and initiation of under frequency load shedding. Using the voltage magnitude at generator buses opposed to rotor angle or frequency in the detection of a power system's proximity to transient instability is proposed in [24] with a 95 percent success rate. In [25] a PMU based technique using the Lyapunov Exponent (LE) is proposed and tested. LEs are used in ergodic theory of dynamical systems to characterize the exponential convergence or divergence of nearby trajectories.

According to IEEE and CIGRE working groups [26] "voltage stability refers to the ability of a power system to maintain steady voltages at all buses in the system after being subjected to a disturbance from a given initial operating condition." From [27] "voltage instability stems from the attempt of load dynamics to restore power consumption beyond the capability of the combined transmission and generation systems." Since synchrophasor based applications for the assessment and detection of voltage stability is the focus of our research we have done a more extensive literature review covered in chapter three.

Creating visualization tools for use in control room applications, which will be the interface between PMU data and system operations, is vital for the optimal use of this data in real-time. There are numerous displays utilized to manage SCADA measurements and state estimation that are already implemented in the control room. Most control rooms have approximately six computer monitors per operator but not all of the displays are viewed at the same time. Adding another display to the mix is something that most system operators are hesitant to accept. This hesitancy makes the task of finding simple visualization tools that are easy to understand, error

free and actionable important for acceptance in the control room.

A proposed example of using a contour map with measurements of phase angle differences across a geographical map is discussed in [28]. Electric Power Group (EPG) has created a Real Time Digital Monitoring System (RTDMS) for use with WAMS technology. It serves as as a tool to translate research concepts and algorithms for use by system operators, operating engineer support and reliability coordinators. It is an open platform that is scalable with a modular system design that offers a suite of applications for visualization, monitoring and alarming on grid stress, dynamics and proximity to instability [29]. This software can be complimented with a post event data analysis tool also produced by EPG called Phasor Grid Dynamic Analyzer (PGDA). Another tool for visualizing and correlating the dynamic attributes of a system using PMU data is proposed in [30]. In this visualization tool, mode frequency, damping, residue (participation factor) and mode energy can be visualized on top of a geographical map. Two types of plot designs are discussed in this thesis: one comprises a set of holistic geospatial visualizations that includes trends and outliers and the second design supports exploration and further analysis. In another paper [31] a real-time visualization tool using hybrid SCADA and PMU measurements is proposed. There are several possible display methods that are discussed including a contour map with colors representing phase angle differences and thermometer type graphics representing voltage magnitude, a grid view with meters showing phase angle differences, one that highlights rapid changes and one that couples with the contingency analysis tool to show worst-case overloads.

PMU measurements can be used in system identification in which a model is constructed from a combination of its outputs and possibly some inputs. System identification can be useful when one does not know the precise physical laws governing the system. For this to be realized in linear time invariant (LTI) discrete time dynamical systems we need to make three assumptions. The system must be controllable and observable, the input needs to be significant enough to "stir" the contribution of the dominant dynamic modes in the output, and there are no future inputs or past states that are affecting the output data [32].

In this analysis we assume that the significant input is an impulse and the initial value of the state of the system is zero. Using this to evaluate the general dynamic state space model leads to a pattern that can be used to develop the Hankel matrix which is realized as the product of the observability matrix and the controllability matrix.

The method above can be applied to estimate the dynamic model and using the state matrix we can extract the different mode frequencies of a system as well as their residue (participation factor) and energy. Power systems are usually divided between fast modes or intra-area modes and slow modes or inter-area modes. These inter-area modes are usually between 0.1 to 1 Hz in frequency and are prominent in the Western Electric Coordinating Council (WECC). Motivation for reduced order dynamic models comes from the fact that conventional model based

equivalencing methods are numerically challenging, time consuming and require precise parameter knowledge [33]. In [33] this information is used to build a simplified electro-mechanical model of the Pacific AC inter-tie consisting of a three area star connected topology. In another paper [3] the information was used to create a simplified equivalent five machine inter-area model of the US west coast grid. One method for identifying the topology for these equivalent models using subspace identification methods is introduced in [34].

There are several applications that use PMU data within protection systems. Traditional protection is closely related to circuit breaker operation that protects faulty or overloaded equipment, people, animals and property from injury and damage caused by electric faults. Wide area or system protection is protection that is used to save a system from a blackout or brown-out situation. In these particular situations there are (not necessarily) individual pieces of equipment that are faulty or overloaded. This can occur when the system is stressed, or operated close to its limits and can actually become worse when traditional protection operates to clear faulty equipment and lines under stressed conditions [35]. Most of the protection applications using PMU data fall under the umbrella of adaptive protection. Adaptive protection can use current prevailing power system conditions to change their characteristic where as traditional protective systems respond in a predetermined manner. Some opportunities for adaptive protection include out of step protection, transformer protection and system restoration. Other protection schemes that can benefit from phasor measurements include differential transmission line protection and distance relaying for multi-terminal or compensated transmission lines [5].

Most control is closely linked to protection systems, in fact this particular section of power systems is typically called protection and control. Traditional protection devices control circuit breakers to clear faulty equipment and protect people. In [35] wide-area control is split between emergency control and normal control. Emergency control describes actions taken to save the power system. Some of these could be actions like boosting the exciter on a synchronous generator, changing the direction of a high-voltage dc connection or fast valving to counteract transient stability. Normal control describes actions taken that are preventative, aiming to adjust the present and near future operating conditions to maintain stability. These can be either discrete actions such as the operation of a tap changer or shunt device or continuous such as frequency control and automatic generation control (AGC). The consequence for the failure of normal control is an increased risk for instability. The consequence for the failure of emergency control is instability. Therefore, the time and reliability response requirements for emergency control is much higher.

1.4 Organization of Thesis

This thesis has been organized as per the following chapters:

- **Chapter 2:** Event Baselining

  The second chapter presents the baselining results surrounding events. For all of the event baselining analysis we looked at data collected from the PMUs installed on the system. First we look at ranges of values for three specific measurements including voltage magnitude, voltage phase angle and frequency. Second we explore baselining around the dynamic slow modes or frequencies of the system using the Eigensystem Realization Algorithm (ERA) implemented in Matlab.

- **Chapter 3:** Voltage Stability Overview

  The third chapter covers an extensive literature review of voltage stability assessment and detection applications using PMU data. From the applications studied we choose two methods, namely the measurement based LE method and decision tree method, to compare. Since there is no actual PMU data surrounding voltage instability we used Power System Simulator for Engineering (PSSE) to create simulation data.

- **Chapter 4:** Voltage Stability Assessment Using The Lyapunov Exponent

  The fourth chapter covers the measurement based algorithm for calculating the LE, and a couple different techniques using the LE in the assessment and detection of voltage stability. In one experiment we try to determine if we can calculate the voltage sensitivity of an unmonitored neighboring bus to a PMU monitored bus as a function of the amount of current on the branch between the two buses. For this analysis we used data from PSSE simulations of the IEEE 9 bus model. In a second experiment we explore the relationship between the characteristic of the LE and the final margin as it relates to system contingencies, operating conditions and proximity to voltage stability load limits. For this analysis we used data from PSSE simulations on Duke Energy's system model.

- **Chapter 5:** Voltage Stability Assessment Using The Decision Tree

  In the fifth chapter we review the efforts between our collaborators at SAS Institute and NCSU in exploring the use of the decision tree data mining technique for the assessment of voltage stability using the SAS Enterprise Miner software suite. The data that we used to build the decision tree came from PSSE simulations on Duke Energy's system model. This chapter reviews the data acquisition process as well as the results from two decision trees. Finally the subset of the contingencies and operating conditions used in the simulations are evaluated using the corridor equivalent impedance technique, creating a power versus voltage (PV) curve and calculating the maximum power transfer and critical voltage for each case.

- **Chapter 6:** Conclusion

The sixth chapter summarizes the PMU data analysis covered in this thesis, reviews the results and draws conclusions based on the results. The first section focuses on the baselining efforts and the second section focuses on the voltage stability assessment. We propose a syncrophasor application in which the results of this study could be used to enhance the situational awareness of voltage stability for system operations. Finally, future work in the area of PMU data analysis, baselining and application exploration is suggested.

Chapter 2

Event Baselining

2.1 Overview of the Duke Energy System

Today Duke Energy is responsible for providing reliable and affordable electricity to approximately 7.1 million customers over approximately 104,000 square miles covering six states shown in Figure 2.1 [36]. Parts of Florida, Indiana, North Carolina, Kentucky, Ohio and South Carolina are under the Duke Energy umbrella. In order to cover this load they own approximately 50 GW of net generation capacity provided mostly by hydro, nuclear, coal-fired, combustion turbine and combined cycle [37]. The Duke Energy territory that this paper is focused on contains approximately 3000 buses with transmission voltages of 500 kV, 230 kV and 100 kV. The Duke Energy owned generation mix includes thirty hydroelectric plants, eight coal-fired steam plants, four combustion turbine plants and four nuclear plants.

Duke Energy's vision for synchrophasor technology was developed in the Summer and Fall of 2010 by a team with members from Transmission Planning, System Operations, Telecom, Energy Management Systems (EMS) Engineering and System Protection. The overall vision requires the integration of synchrophasors into system protection, system planning and system operations. In the Carolinas the plan was to install up to 104 PMUs at 52 substations providing 100 percent coverage of 500 kV buses, 230 kV buses and 500 kV lines as well as 60 percent of 230 kV lines. In addition to the installation of the PMUs they would need to upgrade substation communications, upgrade the EMS and install Phasor Data Concentrators (PDCs). Internal and external subject matter experts determined near term applications which include visualization tools, improved state estimation, system model validation and post event analysis. Longer term applications would include the monitoring of angular separation and voltage stability margin [38].

The Duke Energy territory that is the subject of the PMU data analysis in this project contains 125 PMUs at 58 substations. The PMUs cover all of the 500 kV and 230 kV substations

Figure 2.1: Duke Energy Territory

and are also installed on some lower voltage interconnections. Duke Energy is incorporating EPG's real-time visualization software RTDMS and post event analysis tool PGDA starting with their operations engineering group. They also plan to update the EMS to a version which allows the integration of phasors and are looking into gateway devices to exchange data with external entities.

They have updated much of the substation communication and have installed multiple PDCs for redundancy. Duke Energy's PMUs are Schweitzer Engineering Laboratories (SEL) model 351A and have been configured to get 30 samples of data per second. The PDCs are streaming UDP to centrally processed applications using C37.118 protocol. The PMU data flow is shown in Figure 2.2 [2].

There are 80 TB of storage for PMU data at two different locations. The plan is to have three years of data easily accessible with event data archived for a longer period. There is compression performed on the most of the data except for frequency which in general is approximately half the precision of the measuring device. In total there is about 8 GB of data stored per day 3.5 TB per year [2].

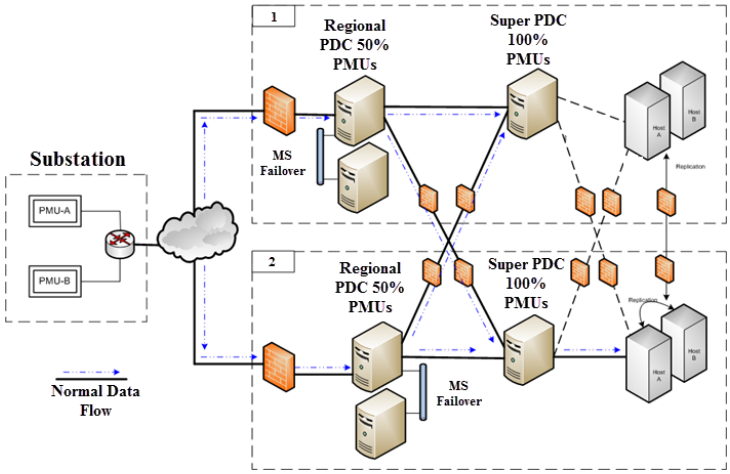

Figure 2.2: PMU Data Flow

In the initial stages of the PMU data analysis we wanted to do some baselining around system events. For our analysis we chose to focus on the thirteen 500 kV PMUs. First we

analyzed ranges of values for frequency, voltage magnitude and voltage phase difference for each PMU across multiple events. Second we analyzed the dynamic slow frequency modes across multiple events for each PMU. A generic model of the 500 kV system is shown in Figure 2.3.

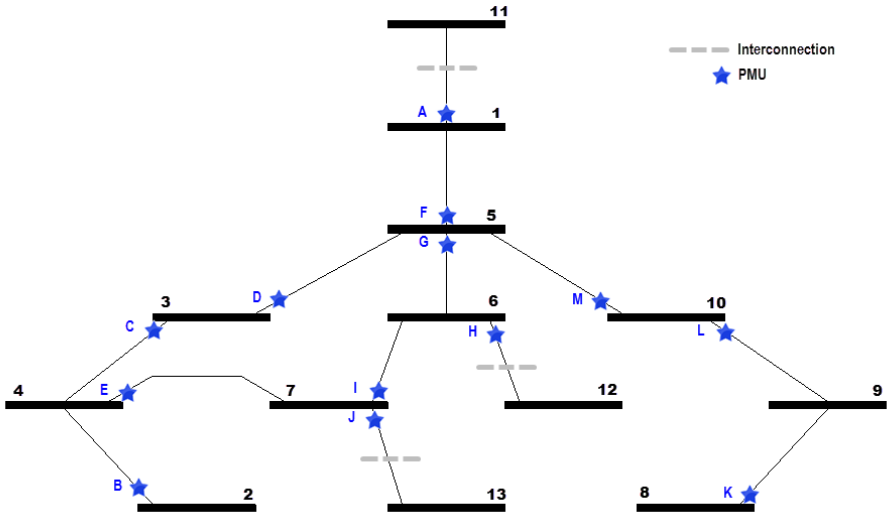

Figure 2.3: 500 kV System Model

2.2 Event Baselining - Range of Values

For this baselining analysis we obtained four minutes of PMU data, starting at one minute before the event, for the four line loss events from the Fall of 2013 shown in Table 2.1. The minimum and maximum values of frequency, voltage magnitude and voltage phase difference were evaluated as well as the variance and standard deviation across all events for each PMU.

In order to compare the data from the four events for a single PMU we plotted the different measurements from 55 seconds to 70 seconds. As expected the PMU closest to the event has the greatest response and the 500 kV PMUs had a greater response from the 500 kV events than the 230 kV event. In Figure 2.4 we can see that the 230 kV event, event number two, has the largest response on the graph for PMU *I* located at bus seven.

Table 2.1: Baselining Line Loss Events

Event	Branch kV	Bus From	Bus To	Time	Notes
1	500	10	9	5pm	
2	230	NA	NA	8am	Closest 500kV bus 7
3	500	8	9	6am	
4	500	8	9	6am	

The same is true for the first 500 kV event. This event has the largest response on the graph for PMU M which is closer to buses 9 and 10 where the line tripped as shown in the following figures. Since PMU L gets its data from the line that tripped it did not record data during this time.

For the voltage magnitude and frequency result summary we converted the values to per unit quantities and plotted the minimum and maximum for each PMU on one chart for voltage magnitude Figure 2.6 and another chart for frequency Figure 2.7. Next we calculated the average minimum, average maximum, variance and standard deviation across all PMUs. For the voltage magnitude the average minimum was 0.93 per unit and the average maximum was 1.09 per unit. For the frequency the average minimum was 0.9993 and the average maximum was 1.0014. For both voltage magnitude and frequency the average values have a small standard deviation.

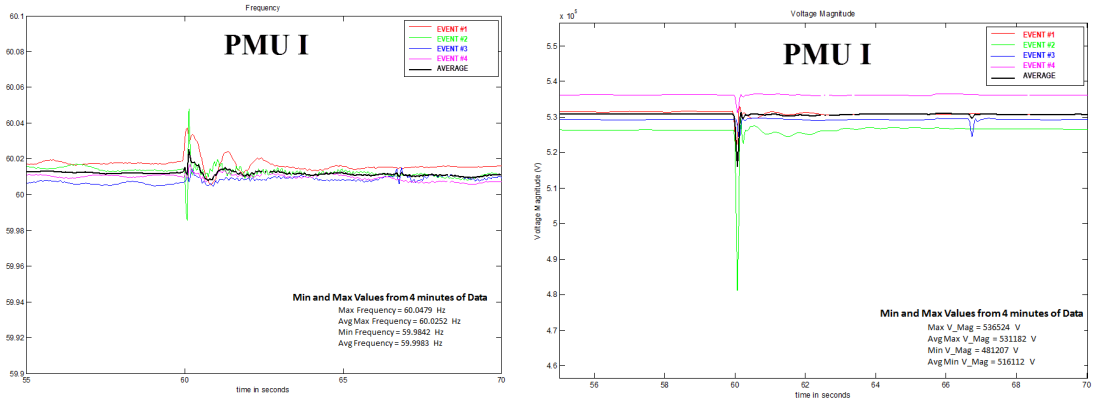

(a) **(b)**

Figure 2.4: PMU *I* (a) Frequency (b) Voltage Magnitude

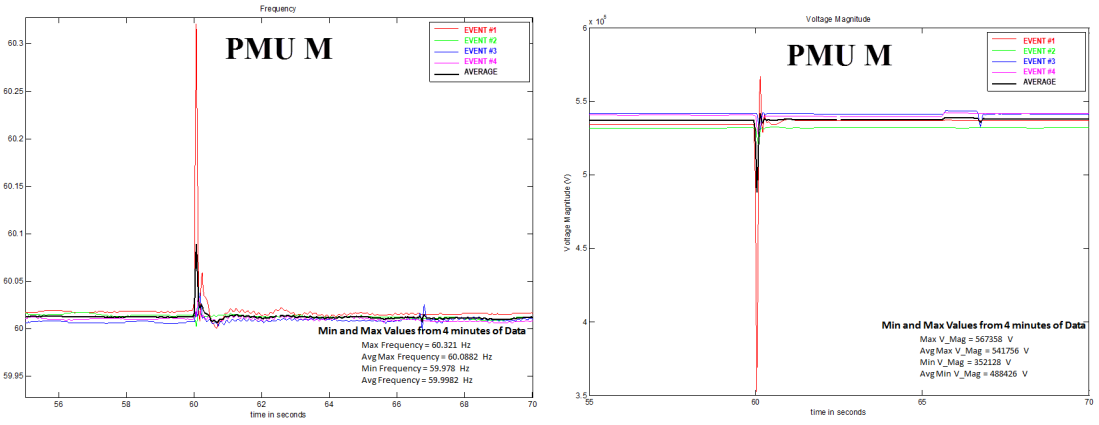

(a) **(b)**

Figure 2.5: PMU *M* (a) Frequency (b) Voltage Magnitude

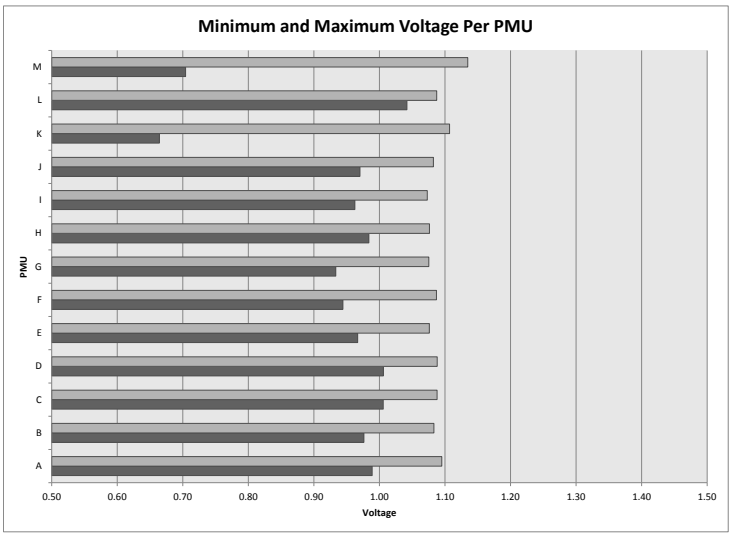

Figure 2.6: Voltage Magnitude

Table 2.2: Voltage Magnitude

	Average	Variance	Standard Deviation
Minimum	0.9345	0.0132	0.1148
Maximum	1.0887	0.0003	0.0166

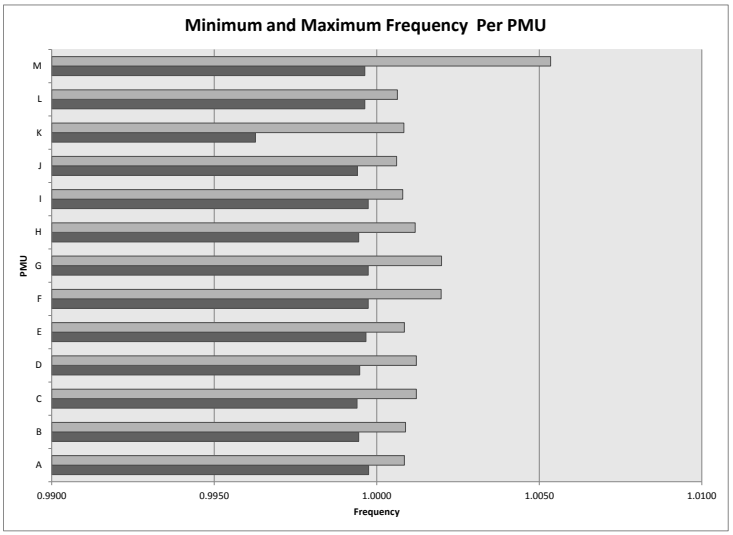

Figure 2.7: Frequency

Table 2.3: Frequency

	Average	Variance	Standard Deviation
Minimum	0.9993	0.000001	0.0009
Maximum	1.0014	0.000002	0.0013

In order to obtain useful information from the PMU phase measurements we needed to come up with a reference phase measurement for comparison and compute the difference between the two. Since it makes the most sense to get the phase difference across a single line and none of the 500 kV lines in the system are tapped we decided to create PMU pairs across each line. Some of the PMUs were used in more than one PMU pair in order to cover all of the lines. With the exception of two lines and the interconnection points we were able to isolate all of the lines. Since there is no PMU at bus nine we had to select PMU L and PMU K which is essentially two lines separated by a bus. Also there is a 500 kV line that goes from one of the buses to a generating station that is not monitored. In total ten PMU pairs shown in Table 2.4 were created.

Table 2.4: PMU Pairs

PMU 1	PMU 2
A	F
B	E
C	E
D	G
G	H
I	H
J	E
K	L
L	F
M	F

The phase difference across a line is a strong indication of the real power transfer across that line as shown by the following power transfer equation where real power is traveling from bus one to bus two and we assume that the resistance of the line is negligible.

$$P = \frac{V_1 V_2}{X} \sin(\theta_1 - \theta_2)$$

When this quantity is negative it can be interpreted that the real power transfer is from bus two to bus one. For stability purposes, we want to keep this angle under 90 degrees, where we hit the maximum power transfer. In the case of a fault we want to make sure that the disturbance doesn't cause the angle difference to approach instability.

For the four events analyzed the greatest angle difference was approximately 9.92 degrees between buses I and H during the first event which occurred at 5 pm. One reason for such small angle differences is that these were all events that occurred in the Fall season, or shoulder month, which is a time where the load (power demand) is minimal. Also, the event that showed the largest angle difference occurred for an event that was during the daily peak load time frame. For this particular study it appears that the heaviest power transfer is between bus I and bus H.

However, the flow of power across a power system depends on several factors. Power flow varies with different generation and load patterns, particularly where the generation is coming from and where the power is being demanded. During a shoulder month power systems complete most of their construction and maintenance projects which alters the amount and location of generation, transmission and distribution resources. Therefore, it is hard to determine if this power transfer pattern would be the same for the Summer or Winter months or during a time when different construction and maintenance projects are taking place. Second, the power transfer across a system depends on the type of load. The difference in the time pattern, the amount, and the type of power demanded can vary between residential, commercial and industrial loads. This is due to the fact that commercial and residential loads fluctuate where industrial loads tend to remain constant. This difference is taken into account in planning and operational studies where the load is incremented. In cases where simulations are performed the industrial load remains constant and the commercial and residential loads are scaled. Third, the power transfer pattern depends on power transactions between different utilities. Every day there is power being sold and bought by different utilities in search of the most economical generation to meet their individual loads. These transactions not only affect the systems of the utilities involved in the ultimate transaction but also affects the utilities in which the power transverses to get to its final destination. There is little control in the flow of power which is mostly governed by system conditions.

On the other hand there were some interesting observations shown in Figure 2.8. During the timing of all events it looks like the power flow between some buses were very similar as is shown for PMU pair G to H, bus five to six, and between other buses were very different as shown for PMU pair I to H, bus seven to six. Similar to the voltage magnitude and frequency, the closer the buses in the PMU pair are to the location of the event the larger the response

in the angle difference. For example the PMU pair J to E, bus seven to four, has the largest response for event two that occurred near bus seven. The PMU pair M to F, bus ten to five, has the largest response for event one that occurred from bus ten to bus nine. Since the PMU pairs are located on the 500 kV buses there is a larger response seen for the 500 kV events than the 230 kV event. For the most part the power continued to flow in the same direction except for the case of the PMU pair M to F, ten to five, for event one occurring between bus ten and nine.

For the result summary we took the absolute value of each phase angle difference in order to evaluate the minimum and maximum quantities. The fact that the angle difference is a negative quantity indicates the direction of power flow, not the fact that it is smaller than a positive quantity. After taking the absolute value we plotted the minimum and maximum for each PMU pair on one chart. Next we calculated the average minimum, average maximum, variance and standard deviation across all PMUs. For the voltage phase angle difference the average minimum was 1.12 degrees and the average maximum was 4.38 degrees. The standard deviation of these average values is much larger than we saw with voltage magnitude and frequency. This is due to the nature of the quantity being measured with respect to the power system.

Frequency is the most highly monitored and controlled characteristic of the power system. This is a measure of how well the load and generation are balanced. If the load is greater than the generation the frequency will fall below 60 Hz. If the generation is greater than the load the frequency will be greater than 60 Hz. Most utilities try to keep this range within 60.05 Hz and 59.95 Hz. Voltage is also a controlled quantity of the power system. Each generator is set up to control a voltage either at the generator bus on the low side to the step up transformer or at the switchyard bus on the high side of the step up transformer. This is accomplished by adjusting the excitation of the generator. Voltage regulators, tap changing transformers, capacitor banks and FACTS devices such as SVCs are all used throughout the system to help maintain an acceptable voltage at every bus. Most utilities try to keep this range between 1.05 per unit and 0.95 per unit. The phase angle difference changes with the power flow on a line. This power flow can vary significantly depending on load, generation, system configuration and other operating conditions. Therefore it makes sense that we would see a larger standard deviation for the phase angle difference average values.

2.3 Event Baselining - Dynamic

Next, we wanted to do some dynamic baselining using either the frequency or voltage phase angle difference characteristic post disturbance to look for slow oscillation modes across the system. This is useful in doing system identification of dynamic models in power systems using measured outputs. In order to determine the modes from the waveform we used the Eigensystem

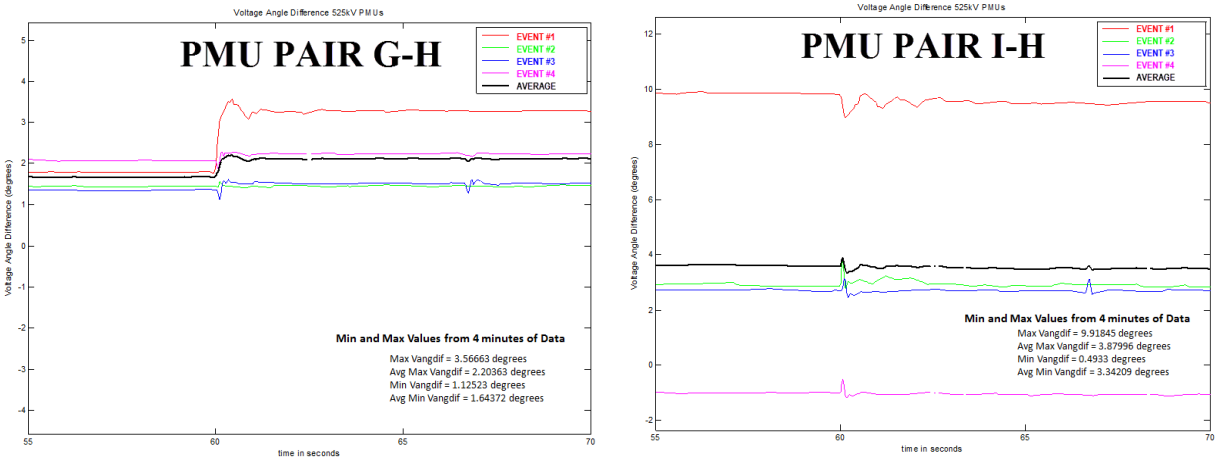

Figure 2.8: PMU Pairs (a) *G-H* (b) *I-H* (c) *J-E* (d) *M-F*

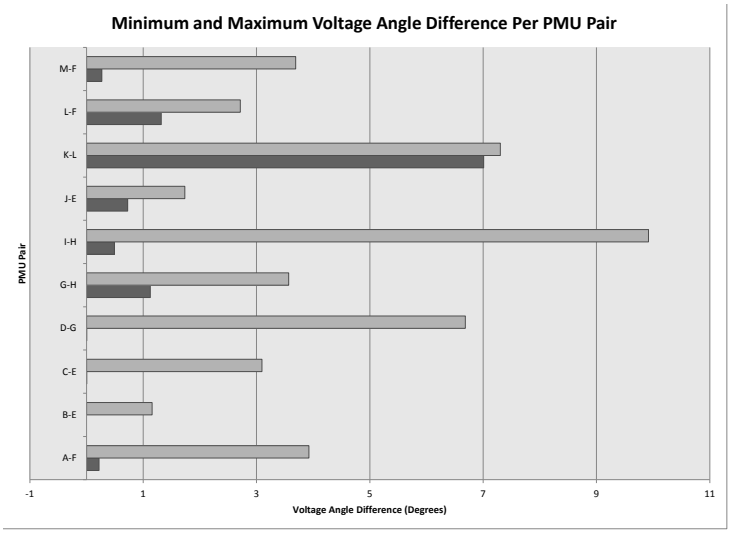

Figure 2.9: Voltage Phase Angle Difference

Table 2.5: Voltage Phase Angle Difference

	Average	Variance	Standard Deviation
Minimum	1.12	4.51	2.12
Maximum	4.38	7.52	2.74

Realization Algorithm (ERA) implemented in Matlab. This algorithm helps solve a general subspace ID problem, a powerful tool for constructing discrete-time dynamic models of large order systems in the time-domain using state variable models [39].

Eigensystem Realization Algorithm (ERA) The following explanation describes the single input single output (SISO) scenario. The actual ERA allows for the analysis of multiple input multiple output (MIMO) as well. Also, we have used information from [32] to better explain the following steps. First we assume that the system can be represented by a LTI discrete dynamical system.

$$x(k+1) = Ax(k) + Bu(k) \tag{2.1}$$

$$y(k) = Cx(k) + Du(k) \tag{2.2}$$

Neither the order of the system or the contents of the matrices (A, B, C, D) above are known. The measured quantity of frequency or voltage phase angle difference is $y(k)$. The algorithm conveniently and appropriately assumes the system was excited by a short lived impulse in discrete time. This is appropriate because most large disturbances resemble an impulse characteristic meaning the disturbance happens at an instant in time and then the system is left to settle back to an equilibrium without any extended input from the disturbance. Therefore for the input we have the following:

$$u(k) = \begin{cases} 1 & \text{for } k = 0 \\ 0 & \text{for all other } k \end{cases} \tag{2.3}$$

Another assumption we have to make to complete the algorithm is that there were no initial conditions, the system was at rest before the input.

$$x(0) = 0 \tag{2.4}$$

In order to illustrate the derivation we start by evaluating the state space model at different values of k.

Iteration 1: $k = 0$

$$y(0) = Cx(0) + Du(0)$$

from 2.3 and 2.4 $x(0) = 0$ and $u(0) = 1$

$$y(0) = D \tag{2.5}$$

Iteration 2: $k = 1$

$$x(1) = Ax(0) + Bu(0)$$

$$y(1) = Cx(1) + Du(1)$$

from 2.3 and 2.4 $u(0) = 1$, $u(1) = 0$ and $x(0) = 0$

$$x(1) = B \tag{2.6}$$

$$y(1) = CB \tag{2.7}$$

Iteration 3: $k = 2$

$$x(2) = Ax(1) + Bu(1)$$

$$y(2) = Cx(2) + Du(2)$$

from 2.3 and 2.6 $u(1) = 0$, $u(2) = 0$ and $x(1) = B$

$$x(2) = AB \tag{2.8}$$

$$y(2) = CAB \tag{2.9}$$

Iteration 4: $k = 3$

$$x(3) = Ax(2) + Bu(2)$$

$$y(3) = Cx(3) + Du(3)$$

from 2.3 and 2.8 $u(2) = 0$, $u(3) = 0$ and $x(2) = AB$

$$x(3) = A^2B \tag{2.10}$$

$$y(3) = CA^2B \tag{2.11}$$

From this pattern we can derive the following general equation. These are sometimes referred to as the Markov Parameters.

$$y(k) = CA^{k-1}B \tag{2.12}$$

Using this we can construct a matrix of the output in the following form, known as the Hankel matrix.

$$H_1 = \begin{bmatrix} CB & CAB & CA^2B & \dots & CA^{M-2}B & CA^{M-1}B \\ CAB & CA^2B & CA^3B & \dots & CA^{M-1}B & CA^MB \\ \vdots & \vdots & \vdots & \vdots & \vdots & \vdots \\ CA^{N-1}B & CA^NB & CA^{N+1}B & \dots & CA^{M+N-3}B & CA^{M+N-2}B \end{bmatrix} \tag{2.13}$$

By observation we can see that the structure of this matrix is equal to the product of the observability and controllability matrices.

$$H_1 = OL \tag{2.14}$$

$$O = \begin{bmatrix} C^T & (CA)^T & (CA^2)^T & \dots & (CA^{N-1})^T \end{bmatrix}^T \tag{2.15}$$

$$L = \begin{bmatrix} B & AB & A^2B & \dots & A^{M-1}B \end{bmatrix} \tag{2.16}$$

Next we take the singular value decomposition (SVD) of the Hankel Matrix to eliminate unnecessary modes contained in H_1. The ERA prompts the user to enter the number of singular values that it should use. The SVD is in the following form.

$$H_1 = \begin{bmatrix} U_1^T & U_2^T \end{bmatrix} \begin{bmatrix} \Sigma_1 & 0 \\ 0 & \Sigma_2 \end{bmatrix} \begin{bmatrix} V_1 \\ V_2 \end{bmatrix} \tag{2.17}$$

Using the number of singular values the user selects the reduced-order Hankel matrix is in the following form. Which can be realized as the product of the observability and controllability matrices in a similar manner.

$$\overline{H_1} = U_1^T \Sigma_1 V_1 = \overline{OL} \tag{2.18}$$

$$\overline{H_1} = U_1^T \Sigma_1^{\frac{1}{2}} \Sigma_1^{\frac{1}{2}} V_1 = \begin{bmatrix} \Sigma_1^{\frac{T}{2}} & U_1 \end{bmatrix}^T \begin{bmatrix} \Sigma_1^{\frac{1}{2}} & V_1 \end{bmatrix} = \overline{OL} \tag{2.19}$$

Next we construct the Hankel matrix starting with the second output as follows.

$$H_2 = \begin{bmatrix} CAB & CA^2B & CA^3B & \dots & CA^{n-1}B & CA^nB \\ CA^2B & CA^3B & CA^4B & \dots & CA^nB & CA^{n+1}B \\ \vdots & \vdots & \vdots & \vdots & \vdots & \vdots \\ CA^nB & CA^{n+1}B & CA^{n+2}B & \dots & CA^{2n-2}B & CA^{2n-1}B \end{bmatrix} \tag{2.20}$$

From the definitions of the observability and controllability matrices we can rewrite this as the product of the observability matrix, the A matrix and the controllability matrix.

$$H_2 = \overline{O} A \overline{L} = \begin{bmatrix} \Sigma_1^{\frac{T}{2}} & U_1 \end{bmatrix}^T A \begin{bmatrix} \Sigma_1^{\frac{1}{2}} & V_1 \end{bmatrix} \tag{2.21}$$

Since we know what our observability and controllability matrices are as well as the second Hankel matrix that we derived we can find our A matrix, the state matrix of the system.

$$A = \begin{bmatrix} \Sigma_1^{\frac{T}{2}} & U_1 \end{bmatrix}^{-T} H_2 \begin{bmatrix} \Sigma_1^{\frac{1}{2}} & V_1 \end{bmatrix}^{-1} \tag{2.22}$$

The eigenvalues of this matrix are responsible for determining the modes of the system.

For the dynamic analysis of the Duke Energy system we collected 15 seconds of data from 19 events. This included 5 seconds pre disturbance and 10 seconds post disturbance. We used frequency since this measurement produced more pronounced oscillations than voltage phase angle difference. Since the ERA algorithm requires the disturbance to have a certain level of severity in order to correctly identify the modes we scanned each event for the disturbance by evaluating the change between samples to be between some range, ϵ_1 and ϵ_2 . If all of the PMUs saw the event at the same time we assumed the disturbance was significant enough for evaluation. If not all of the PMUs saw the event at the same time we did not use the data in our analysis labeling it as a poorly identified event. Also if the data had data quality issues, such as frequency values that were missing or zero we were unable to use the data. Finally we took the remaining four events and ran 10 seconds worth of data post disturbance through the ERA program in Matlab, recorded the modes that were less than 1 Hz along with their damping. Of the four events one was a generation loss event and three were line loss events. The location and times of the events are included in Table 2.6.

Table 2.6: Dynamic Baselining Events

Event Number	Event Type	kV	Bus From	Bus To	Event Time
1	Line Loss	500	8	9	6am
2	Generation Loss				1pm
3	Line Loss	500	8	9	8pm
4	Line Loss	500	Not Shown	10	10pm

The results are shown below. Although the disturbances for all four events were seen across all of the PMUs there were many data sets that had data quality issues such as missing or incorrect values for certain PMUs. Therefore, most of the PMUs are missing results for some of the events.

Table 2.7: PMU *A*

Event Number	Frequency	Damping
1	0.6905	0.1864
2	0.6018	0.3040
3	0.4902	0.3787
4		

Table 2.8: PMU *B*

Event Number	Frequency	Damping
1	0.7153	0.2889
2	0.7921	0.4367
3	0.8451	0.3321
4	0.8673	0.8051

Table 2.9: PMU *C*

Event Number	Frequency	Damping
1	0.6538	0.2258
2		
3	0.8816	0.2983
4		

Table 2.10: PMU *D*

Event Number	Frequency	Damping
1	0.6671	0.2202
2		
3	0.8576	0.3102
4		

Table 2.11: PMU *E*

Event Number	Frequency	Damping
1	0.7022	0.2499
2		
3	0.8604	0.3385
4		

Table 2.12: PMU *F*

Event Number	Frequency	Damping
1		
2	0.8676	0.4464
3	0.8914	0.2972
4		

Table 2.13: PMU *G*

Event Number	Frequency	Damping
1		
2	0.8730	0.4765
3	0.8765	0.2894
4		

Table 2.14: PMU *H*

Event Number	Frequency	Damping
1	0.6670	0.2175
2	0.5535	0.6842
3	0.7838	0.3097
4		

Table 2.15: PMU *I*

Event Number	Frequency	Damping
1	0.7307	0.3700
2	0.7878	0.3539
3	0.8541	0.2383
4		

Table 2.16: PMU *J*

Event Number	Frequency	Damping
1	0.7113	0.3388
2		
3		
4		

Table 2.17: PMU *L*

Event Number	Frequency	Damping
1	0.6277	0.1648
2		
3	0.6987	0.1912
4		

Table 2.18: PMU *M*

Event Number	Frequency	Damping
1	0.6275	0.1575
2	0.6134	0.4830
3		
4		

The following bar chart summarizes the results. Each light grey (frequency) and dark grey (damping) pair indicate a particular PMU for a particular event. The PMU letter is shown on the chart and the events are in numerical order according to the events that were evaluated for each PMU which can be determined by looking at Table 2.7 through Table 2.18. The modes ranged from 0.4902 Hz to 0.8914 Hz with an average of 0.7431 Hz. The median was close to the average at 0.7230 Hz and the average value had a minimal standard deviation. When rounded to the second decimal place the modes that are repeated the most, three times in the data, were 0.63 Hz and 0.87 Hz. Although it appears that the results showed modes within a limited range there was not a significant enough repetition of a single mode to determine the accuracy.

This could be due to the fact that there was not enough good data to evaluate. However, since slow modes are indicative of oscillations between two areas separated by a long power transfer path and the Eastern Interconnection is a highly meshed system there may not be any easily defined slow modes.

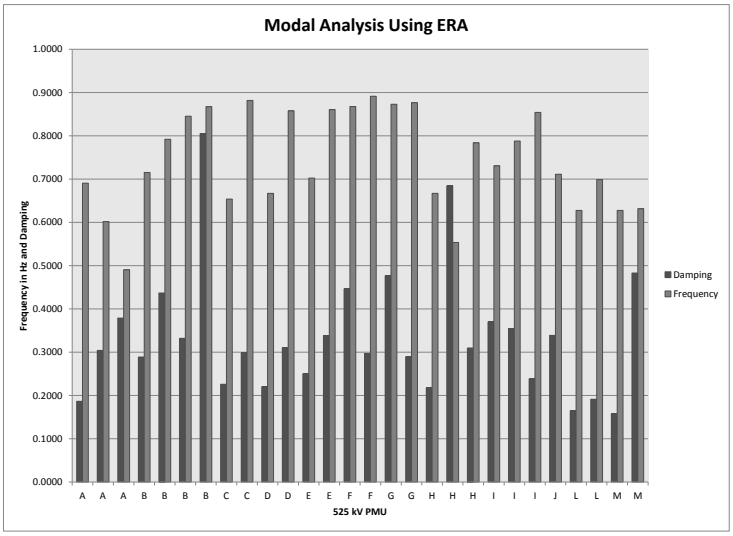

Figure 2.10: Mode Frequency and Damping Per PMU Per Event

Table 2.19: Mode Frequency and Damping

	Minimum	Maximum	Average	Median	Variance	Standard Deviation
Frequency	0.4902	0.8914	0.7431	0.7230	0.0127	0.1127
Damping	0.1575	0.8051	0.3355	0.3069	0.0211	0.1451

Chapter 3

Voltage Stability Overview

There has been increasing focus on the assessment of voltage stability recently. According to IEEE and CIGRE working groups [26] the ability of a power system to maintain an appropriate steady voltage at all buses after a disturbance is defined as voltage stability. The recent attention to voltage stability can be attributed to the fact that in the past many utilities invested a large amount in capital, such as generation, transmission and distribution assets, making the system's capacity much larger than the demand required. However, as economic pressures have increased, the trend has changed to a more conservative approach causing the margin between demand and capacity to narrow. From [27] load dynamics attempt to restore power to a load beyond the capability of the power systems generation, transmission and distribution capacity can result in voltage instability. Therefore the likelihood of voltage instability has increased.

Power system stability can be divided under two types of classification, first being generator-driven versus load-driven and second being short-term versus long-term. Voltage stability falls under both the short-term and long-term load-driven classifications [27]. Long-term voltage stability is a function of the electrical distance between generation and loads which ultimately depends on the structure of the network at any given time[27]. Long-term voltage stability can be analyzed using an equivalent impedance and an equivalent generation source voltage at the load bus and calculating the relationship between power and voltage. The most famous form of this relationship is the real power versus voltage curve also known as the PV curve which can be realized through the Thévenin impedance matching technique. The driving force behind long-term voltage instability post contingency is the system's attempt for load power restoration such as Load Tap Changers (LTC) coupled with the system's maximum power being reduced by generator reactive power limits enforced by Over Excitation Limiters (OEL) [40].

Short-term voltage stability is closely coupled to dynamic load components, mainly induction motors and electronically controlled loads. When the power that these loads consume is depressed or interrupted they will try to restore their consumed power in the time frame of

one second [27]. Short-term voltage instability most often results from the fact that induction motors can stall in reduced voltage scenarios, caused by system disturbances, and under these conditions, can draw up to six times their nominal reactive power [41]. Analysis of short-term voltage stability is not as straight forward as long-term voltage stability analysis. Not only does short-term voltage stability assessment rely on system conditions and contingency location but also on accurately modeling aggregate load dynamics. Both long-term and short-term voltage instability can lead to voltage collapse, where a sequence of events leads to abnormally low voltage over a large area of the system or a complete blackout [1]. Table 3.1 lists several voltage collapse incidents that occurred between 1995 and 2009.

Another voltage-related phenomenon that can occur is known as Fault Induced Delayed Voltage Recovery (FIDVR). "FIDVR is a voltage condition initiated by a transmission, subtransmission, or distribution fault and characterized by the stalling of induction motors, initial voltage recovery after the clearing of the fault to less than 90 percent of precontingency voltage, and a slow voltage recovery lasting more than two seconds to expected postcontingency steady-state voltage levels" [1]. If the FIDVR event is severe enough it has the possibility of causing voltage collapse. Some important factors regarding this phenomenon are (1) the greater the initial drop in voltage the more reactive power the motor loads demand and (2) the recovery of the voltage depends on the local reactive power support of the system.

3.1 Voltage Stability Literature Review

Our first task is to explore literature on the assessment, detection and control techniques using PMU data for each of the aforementioned voltage phenomenon. We will start with long-term voltage stability since this phenomenon has been explored the most in literature. The detection methods for long-term voltage stability using real time measurements have been summarized and organized in [40]. These methods have been split among methods using wide-area versus local measurements and non-synchronized (i.e. SCADA) versus synchronized (i.e. PMU) measurements. Although this is not an exhaustive list we have used it to organize the following literature review section for long-term voltage stability. There has been considerably less literature that consists of using PMU data for the assessment, detection and control of short-term voltage stability.

3.1.1 Long-Term Voltage Stability

Local Measurement Based Methods

There are two main techniques that fall under the category of local measurement based long-term voltage stability detection. There is the Thévenin impedance matching technique that can

Table 3.1: Voltage Collapse Incidents 1995-2009 [1]

Date	Location	Time Frame	Load Lost	People Affected	Cost
11/11/09	Brazil/Paraguay	68 sec	24,731 MW	87 million	
6/12/04	Greece	30 min	9.000 MW	5 million	
9/23/03	Sweden/Denmark	7 min	6,550 MW	4 million	$75 mil
8/14/03	US/Canada	39 min	63,000 MW	50 million	$7-10 bil
5/97	Chile	30 min	2,000 MW		
8/10/96	Western US	6 min	30,500 MW	7.5 million	
6/8/95	Israel	19 min	3,140 MW		

be calculated using non-synchronized measurements or synchronized measurements of voltage and current as well as the LIVES technique that uses non-synchronized measurements [40]. Impedance matching is a way of calculating the maximum deliverable power at a load bus. Given the Thévenin equivalent of the system at the load bus shown in Figure 3.1 combined with our knowledge from circuit theory the maximum power transfer occurs when the apparent impedance of the load is equal to the Thévenin impedance of the system. The LIVES technique attempts to incorporate the effect of the LTC's attempt to restore load in the assessment of long-term voltage stability. In our review we will focus on the techniques that use synchronized measurements specifically impedance matching.

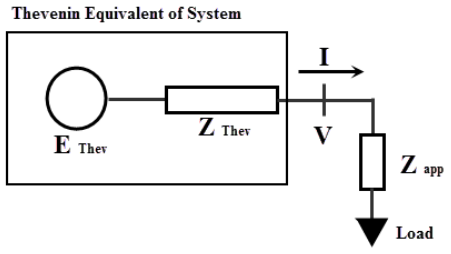

Figure 3.1: Impedance Matching Illustration

A voltage stability risk indicator based on real time adaptive identification of the Thévenin voltage E_{Thev} and impedance Z_{Thev} using recursive least-squares identification from local voltage and current phasors is proposed in [42]. Another application using the Thévenin equivalent via recursive least-squares method is shown in [43]. A device proposed in [44] uses bus voltage and load current to calculate the strength of the system at a particular bus. As the load approaches this value collapse occurs. This is referred to as Stability Monitoring and Reference Tuning Device (SMARTDevice) and experimentally was shown to have less misoperations when compared with the traditional undervoltage relay.

A popular Thévenin impedance technique, the Voltage Instability Predictor (VIP), is reviewed in [45]. In this method voltage and current phasors are used to determine the Thévenin parameters of the system. A new measure, power margin is introduced to the traditional VIP in [46]. Since the VIP method expresses the proximity to voltage collapse in terms of the distance between two voltage curves or two impedance curves it can be difficult to interpret by a system operator. The power margin expresses this in terms of the power that can be pushed through a VIP location before collapse.

Much of the literature is based on impedance matching and uses PMU data and curve fitting tools such as least squares in order to determine the Thévenin parameters at the load bus of interest. However, in [47] a method is proposed to find these Thévenin parameters using the Tellegen's theorem which is computationally less expensive. This theorem only depends on Kirchhoff's laws and network topology. However the computation of these parameters using this theorem requires PMU measurements at consecutive buses.

Wide-Area Measurement Based Methods

Wide-area measurement based methods for assessing long-term voltage stability can also fall under non-synchronized and synchronized based measurements. Non-synchronized measurements of power and voltage can be used in data mining methods such as decision trees as well as other techniques that monitor reactive power reserves [40]. The synchronized measurement based methods are further split into the types of PMU placement methods in [40]. There are three location schemes that are considered. First we consider methods in which the PMU's are properly located for the purpose of voltage instability detection. Next we consider the methods assuming that PMU's are placed appropriately for system observability. Finally we consider the methods based on scarcely placed PMUs, placed appropriately for state reconstruction.

Most of the detection methods fall under the first consideration in which the PMUs are properly located for this purpose. First there are the data mining methods such as decision trees using synchronized phasor measurements. In [48] results of a study for an on-line voltage security monitoring system in AEP using decision trees is explored. This method focuses on

using phase angle differences as the main attribute for the decision tree since it can be directly measured by the PMUs.

One of the techniques that uses PMU data from PMUs that are appropriately placed is the corridor VIP. This technique avoids calculating the Thévenin equivalence of a complete system at one bus by defining a transmission corridor. This method is introduced in [49]. By narrowing the voltage stability assessment to major transmission corridors this technique looks at the power transfer between a source bus and a sink bus. Therefore it is possible to just find the Thévenin equivalent between the buses, the corridor, and the equivalent generation at the source bus. With this method approximate stability margins with an update rate of less than a second have been achieved.

Next the multiport Thévenin equivalent focuses on preserving generation and load information in the area of interest instead of lumping them all into a Thévenin equivalent. In [50] a method is proposed to determine the proximity to voltage collapse based on load characteristics and simulated PMU voltage and current phasors. As the proximity to collapse narrows reactive power reserves are assessed and implemented. Once reserves are exhausted control measures freeze load tap changers and as a last resort sheds load at the particular load bus and other buses in the vicinity. This method can also be realized using what is known as the L-index which was introduced in [51] before the presence of WAMS technology but has been adapted for its use. The L-index is realized by the equations (3.1), (3.2) and (3.3) summarized in [52].

First, from the Kirchoff's Law we have the voltage and current injections at system nodes.

$$I_{system} = \begin{bmatrix} I_L \\ I_G \end{bmatrix} = \begin{bmatrix} Y_{LL} & G_{LG} \\ Y_{GL} & Y_{GG} \end{bmatrix} \begin{bmatrix} V_L \\ V_G \end{bmatrix} = Y_{bus} V_{system} \tag{3.1}$$

Next we rearrange (3.1) to write

$$\begin{bmatrix} V_L \\ I_G \end{bmatrix} = \begin{bmatrix} Z_{LL} & F_{LG} \\ K_{GL} & Y_{GG} \end{bmatrix} \begin{bmatrix} I_L \\ V_G \end{bmatrix} \tag{3.2}$$

The L-index, equation (3.3), at the j^{th} load bus is one minus the sum of all of the F_{LG} terms from all the generators related to the j^{th} load bus multiplied by the voltage at the generator divided by the voltage at the load bus. This ranges from zero during no load conditions to unity at maximum load conditions.

$$L_j = |1 - \sum_{i}^{nG} F_{ji} \frac{V_i}{V_j}| \tag{3.3}$$

In [53] an algorithm for voltage stability monitoring using the L-index is proposed. In [52] the L-index is combined with a neural network data mining technique to assess voltage

stability. The VIP++ method introduced in [54] is an extension of the VIP method in which measurements from multiple buses are used to detect voltage stability.

For situations in which there are enough PMUs for linear state estimation the states of the system can be determined. Examples of stand alone linear state estimation using PMU data only as well as hybrid SCADA and PMU data techniques are reviewed in the general PMU application section of the first chapter. When there are not enough PMUs installed to make the system fully observable it may be desired to apply state reconstruction proposed in [55]. Using the system states obtained by either of the aforementioned methods any of the above wide-area voltage stability detection techniques can be used. A new dynamic voltage stability prediction algorithm using a reduced model and PMU data is proposed in [56].

Some other interesting techniques for assessing and detecting long-term voltage stability not covered in the previous mentioned survey are described here. In [57] the properties of sensitivities to voltage stability and their behavior around the maximum load power are assessed with the purpose of devising a wide-area criterion for detecting long-term voltage instability from bus voltage phasors. A data mining technique, artificial neural network (ANN), is proposed for estimating long-term voltage stability margin in [58]. This technique uses a load P margin, defined as the difference between the maximum power and minimum power consumed by a load, estimating the loading and generation direction and training the artificial neural network through simulations. A method that relates voltage stability properties to the gain margin and phase margin of classic control theory is proposed in [59]. The gain margin is the distance between the load bus voltage at the nose of the PV curve and the top portion of the curve at a given operating point and the phase margin is 90 degrees minus the angle of the line tangent to the top of the PV curve at a given operating point.

3.1.2 Short-Term Voltage Stability

As stated before there has been increased concern regarding short-term voltage stability due to the recent penetration of induction motors and electronically controlled loads. The main cause of short-term voltage instability is the stalling of induction motors following a contingency and can result in voltage collapse within a few seconds. Much of the research in this area focuses on incorporating accurate dynamic models of aggregate fast acting load components in offline simulations [41]. However, in this literature review we focus on methods using PMU data in real-time. A method that proposes determining the steady-state equilibrium post fault by using a reduced model and neglecting the short-term transients in order to detect short-term voltage instability is proposed in [60]. Although this has the advantage that the stability can be indicated directly after the contingency, during the transients, if no equilibrium is found it only leaves the time from which the calculation was complete until the expected occurrence of voltage

collapse to implement a corrective action. This may be of use for long-term voltage stability which can take several seconds to minutes but would be difficult to impossible to resolve with short-term voltage stability in the absence of automatic control. A method using a time series measurement based method to calculate the LE of the voltage magnitude at the bus is proposed in [61]. The LE measures the average rate of expansion or contraction of nonlinear dynamical systems. For stable steady state behavior contraction must outweigh expansion. The Maximum LE (MLE) has been more popularly used in the detection of transient stability. Finally there is the decision tree method proposed in [62] in which simulated PMU data from a combination of operating conditions and contingencies is obtained. The data is separated into secure and insecure classifications in which the decision tree algorithm keeps track of and creates rules that surround data characteristics suggesting either a secure state or an insecure state. These rules are implemented with real PMU data and coupled with an indication of stability, either secure or insecure.

3.2 Techniques for Voltage Stability Analysis Using PMU Data

In this thesis we have focused our application research on using PMU data to assess short-term voltage stability. Not only do we want to be able to detect instability but we want to allow time for operators to process the alarm and take corrective action since the most effective corrective action to prevent short-term voltage instability from voltage collapse is to shed load. Therefore, it is desired to detect situations in which short-term voltage instability would occur a contingency in advance (N-1 condition). Since short-term voltage stability post contingency is a dynamic phenomenon that relies heavily on induction motor load dynamics, in can't be added to a traditional steady state contingency analysis.

Although there have been several ways that have been proposed and studied to help assess voltage stability most of them have been based on long-term voltage stability assessment and current conditions. Here we compare two measurement based methods for the short-term voltage stability assessment of a voltage sensitive area in the Duke Energy System, a method based on the LE and a data mining method using the decision tree. In addition we explore a model based method using a Thévenized equivalent corridor model for the voltage sensitive area in order to assess the validity of chosen operating conditions and contingencies. Since there is no system PMU data surrounding voltage instability we used PSSE to simulate PMU data for our analysis.

First, we looked at the LE based method since it would require the least amount of work to implement. A simple measurement based method for obtaining the LE was presented in [61]. We used this tool initially to determine if there was a relationship between the exponent at neighboring buses. The data evaluated came from PSSE simulations on the IEEE 9 bus system

with complex load models incorporated. If there was a specific and measurable correlation voltage stability beyond monitored buses could be determined. Since voltage stability is a concern at the lower voltage load buses in which minimal PMUs have been placed extending our visibility of the systems voltage stability during a disturbance would be useful. In addition, we wanted to see if this tool could be used to assess how close a particular bus is to voltage collapse at a given operating condition. For this analysis we used data from PSSE simulations on Duke Energy's system model. The plot of this exponent over time settles to a particular final margin. Our hypothesis was that the final margin would decrease as the system reaches a load level in which a particular contingency would cause voltage collapse.

Second, we explored the decision tree based method. For this analysis we used data from PSSE simulations on Duke Energy's system model. Our hypothesis is that there would be common signatures in the steady state PMU data before a given contingency that would cause voltage collapse. The decision tree would be able to create rules that may be used to scan the PMU data in real-time and alert the operators when they are in a vulnerable state given the N-1 contingency would occur. This would not only alert them to a vulnerable state but give them information on the contingency that may cause voltage collapse. We chose these two methods to evaluate because they would be computationally less expensive than other methods, which would save both time and processor resources, and would be reasonably easy to implement.

For all of voltage stability analysis we used PSSE simulation data from either the IEEE 9 bus system model, sensitivity analysis, or the Duke Energy system model, LE matrix and decision tree. When using the Duke Energy system model we specified output from all of the buses and lines where PMUs are placed in a voltage sensitive region. Since PSSE uses a single phase representation of the system we assume that this is equivalent to the positive sequence measurement from the PMUs.

3.2.1 Lyapunov Exponent

The LE of a nonlinear dynamic system characterizes the exponential rate of convergence or divergence, contraction or expansion, of two nearby trajectories. In other words they are a measure of the sensitive dependence chaotic systems have on initial states [63]. These exponents have proven to be a useful dynamical diagnostic for chaotic systems. If the system contains one positive LE it is defined as chaotic with the time scale to unpredictability being proportional to the magnitude of the exponent [64]. "In context of nonlinear dynamics, chaos means long-term irregular or random but bounded trajectories in a deterministic dynamical system which are very sensitive to initial conditions" [63]. An unpredictable trajectory is chaotic even though a set of equations determines how it evolves. If we assume that the convergence or divergence is exponential we can express a single term in the LE spectrum (λ) as shown in equations (3.4)

and (3.5) [65].

$$d(f^n(x_0), f^n(x_0 + \Delta x_0)) = e^{\lambda n} d(x_0, x_0 + \Delta x_0) \tag{3.4}$$

$$\lambda = \frac{1}{n} ln \left[\frac{d(f^n(x_0), f^n(x_0 + \Delta x_0))}{\Delta x_0} \right] \tag{3.5}$$

where Δx_0 is an infinitesimally small distance from x_0 and n is the iteration.

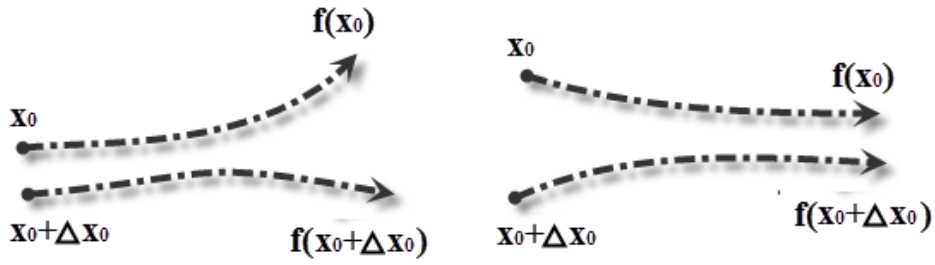

Figure 3.2: Lyapunov Exponent Illustration: Converging and Diverging Trajectories

Following a large disturbance in a power system its transient behavior can be considered chaotic. Therefore, there have been many attempts to use this tool to assess system stability. Since the implementation of PMUs in power systems there have been attempts to calculate the LE using time-series data. In [63] they propose a computer method to detect transiently chaotic swings from real-time PMU data by using the largest LE in a given window of time as an index. Here they define transient chaos in a given window of time when the characteristic of the transient swing is the same as chaos over the entire window. In [61] an algorithm for computing the LE from PMU time-series data is used to determine short-term voltage stability.

3.2.2 Decision Tree

Data Mining has become an increasing popular method of analysis as our increasing capabilities in data acquisition and storage has grown. This specialized field identifies patterns in data using computer aided tools. There are three main types of data mining. First their are ones that base

their analysis on traditional statistical techniques, linear regression and hypothesis testing. The second more modern category was born out of investigation in cognitive science and aims to imitate the human brain. The third focuses on cluster analysis which focuses on grouping a set of objects based on similarities [66].

The decision tree is a data mining technique that uses tools from both the statistical and the cognitive types. There are several useful features that are highlighted in [66]. Most importantly decision trees are simple to produce, understand and use. Decision trees can also incorporate several levels of measurements such as various types of quantitative measurements and qualitative characteristics. It can adapt to data sets with non-linearities, interactions and unbalanced effects. Finally, since it is non parametric it is robust to data quality issues such as missing data.

A decision tree is built from the top down with the base node at the very top. This node contains the entire data set, and in SAS Enterprise Miner will have characteristics of the data such as the total count and the percent of the data in which the target value was realized. The target value is the data field that is the object of analysis. For example, if we were curious to find out what makes someone who starts their studies in electrical engineering finish their degree successfully, all of the students who started the program would be the total count of the data and the data field that stated the status of graduation would be the target. Discovery of the decision tree rule forms the branches under the initial node. This rule is based on a method that extracts the strongest relationship between the target and one or more other data fields from the node in which the branches extend [66].

Chapter 4

Voltage Stability Assessment Using The Lyapunov Exponent

The main goal of analysis using the LE is to determine if this tool can provide useful information for system operations. In this chapter we review two possible methods of voltage stability assessment using the LE. First, we evaluate if the LE can be used to indicate a level of stability at buses neighboring PMU buses as a function of the current on the line. We will refer to this as "Sensitivity Analysis". Since current is one of the measurements obtained by the PMU, if this relationship exists it can be calculated in real-time and provide an extra layer of visibility for operations. This would be particularly useful for voltage stability assessment since voltage instability originates at low voltage buses which typically have less PMU coverage. There are also a greater number of low voltage buses, so extending the visibility of a single PMU for voltage stability assessment would save money, time, communication resources and storage space.

Second, we have evaluated the LE as a tool that would predict the relative stability of a system by analyzing the physical characteristics of the spectrum and ultimately the final margin. If we calculate the LE after an event in which the voltage recovers but at a load level prior to that which would result in voltage collapse, are there components of the plot characteristic or final margin that would indicate this? For both of these assessments we have used an algorithm introduced in [61] to calculate the LE using time series data.

4.1 Lyapunov Exponent Algorithm

Algorithm 1 calculates the contribution of a single bus towards the LE from the time series PMU data given equation (4.1) [61].

$$\frac{1}{Nk\Delta t} \times \sum_{m=1}^{N} \log_{10} \frac{|v^i_{(k+m)\Delta t} - v^i_{(k+m-1)\Delta t}|}{|v^i_{m\Delta t} - v^i_{(m-1)\Delta t}|}, k > N \tag{4.1}$$

For the sensitivity analysis we obtain the LE at both the bus with the PMU and its neighboring bus. This data comes from PSSE simulations on the IEEE 9 bus system with complex load models incorporated. For the characteristic matrix we evaluate the LE at a single bus in the center of a voltage sensitive area. The data for this analysis comes from PSSE simulations on Duke Energy's system model.

Algorithm 1 Measurement Based Lyapunov Exponent Single Bus Contribution

import voltage magnitude PMU data
$n =$ length of data
define e_1, e_2 ▷ lower,upper limit of Δv for transient
define M ▷ number of samples evaluated
define run ▷ minimum number of samples in initial transient
$j = 1, N = 1$ ▷ set counters N will be number of samples in initial transient
for $i = 2, n$ **do**
    if $e_1 < \|v(i) - \bar{v}(i-1)\| < e_2$ **then** ▷ check for delta V between e_1 and e_2
        $N \rightarrow N + 1$ ▷ increment counter for transient values
    else if $N > run$ **then** ▷ check if enough samples for initial vector
        $start = j$ ▷ set start to sample at beginning of transient
        exit for loop
    else$j \rightarrow j + N$ ▷ increment counter
        $N = 1$ ▷ restart count for transient values
    end if
end for
$j = 1$ ▷ set counter
for $k = start + N + 1, start + N + 1 + M$ **do**
    for $m = start + 1 : start + N$ **do**
        $term = \log_{10}\left(\frac{\|v(k+m) - \bar{v}(k+m-1)\|}{\|v(m) - \bar{v}(m-1)\|}\right)$
        $sum \rightarrow sum + term$ ▷ calculate summation term
    end for
    $\lambda(j) = (\frac{1}{Nk\Delta t}) * sum$ ▷ calculate j^{th} element of exponent
    $j \rightarrow j + 1$
end for

The initial transient of the signal is detected when the change in voltage magnitude between samples falls within a certain range between ϵ_1 and ϵ_2. From the beginning of the transient it records all of the voltage magnitudes until the change between two samples falls outside of this range. This is the initial sample that makes up the first trajectory. Next a sample made up of the same number of measurements directly following the first sample is recorded. After these first two samples are recorded we take the logarithm of the ratio in two consecutive measurements of the second sample over the first sample. This is repeated for the 2^{nd} and 3^{rd} measurement in the sample and so forth until all of the logarithms in the initial two samples are calculated are calculated. The sum of these terms divided by the duration of the sample is a single LE.

If this number is positive it suggests that the system is chaotic or unstable and if the number is negative it suggests the system is stable. A simple way to look at the algorithm and how the sign is an indication of stability is by looking at the quotient. If the differences between measurements in the transient (denominator of the quotient) is larger than the differences between measurements in the next sample after the transient (numerator of the quotient) the resulting number is between zero and one. The logarithm of a number between zero and one is negative as can be seen by a simple plot of $\log x$. This would suggest the second sample post transient has less change than the initial transient which would indicate that the transient is damping. If the differences between measurements in the next sample after the transient is larger than the initial transient the value of the quotient is greater than one and the logarithm is a positive value. This would suggest the transient is growing.

Not only does the algorithm compare the next set of measurements equal to the sample size determined by the transient it shifts the sample by one measurement at a time and compares each of these to the initial transient. Therefore the result is a series of LEs for a given amount of time, or M number of samples. The sign and value would fluctuate during the evaluation but in the following results settle to an appropriate sign before five seconds.

When testing the algorithm on real PMU data from an event (event number three from Table 2.6) we were able to get an appropriate negative value and the final margin narrows as the PMU of the data that was evaluated was electrically closer to the disturbance as shown in Figure 4.1. The Event was from bus eight to bus nine from Figure 2.3. The following graphs show the LE and its final margin for four PMUs. PMU B being the farthest from the disturbance and PMU L being the closest to the disturbance.

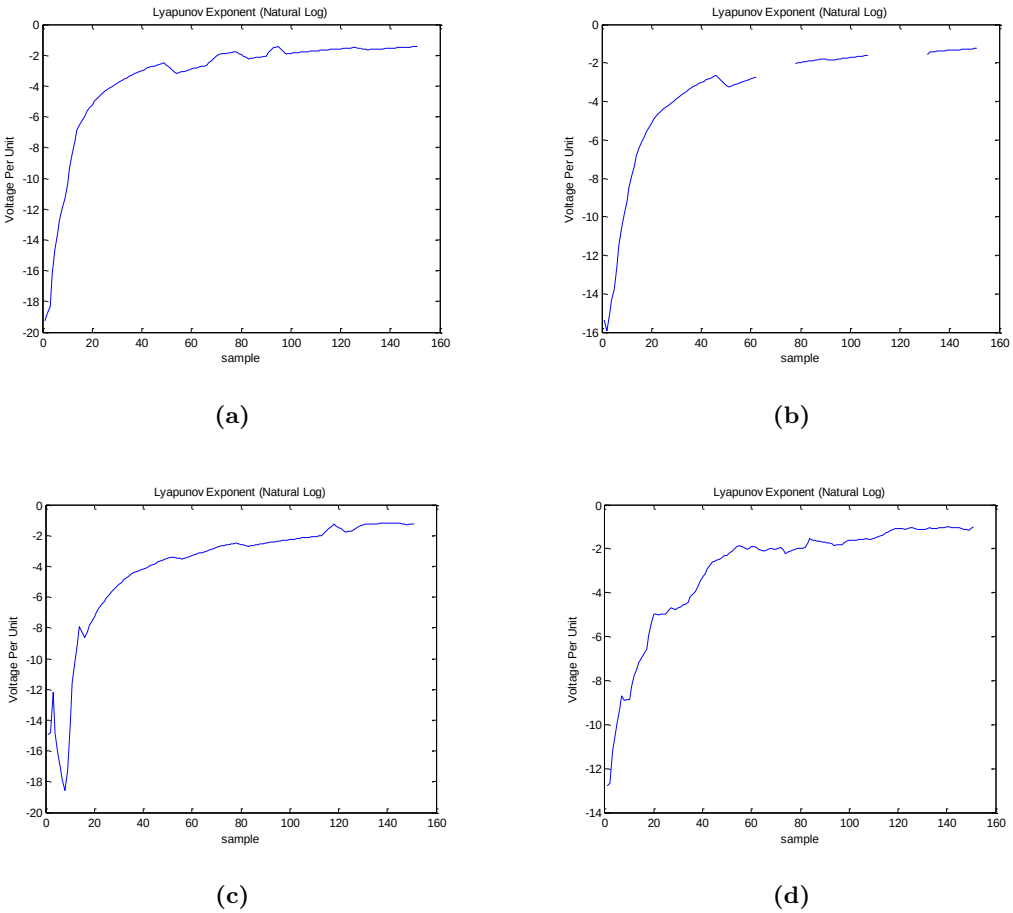

Figure 4.1: LE (a) PMU B (b) PMU C (c) PMU A (d) PMU L

Table 4.1: LE Event Three Final Margin

PMU	B	C	A	L
Bus	2	3	1	10
Final Margin	-1.4389	-1.2504	-1.1747	-1.0058

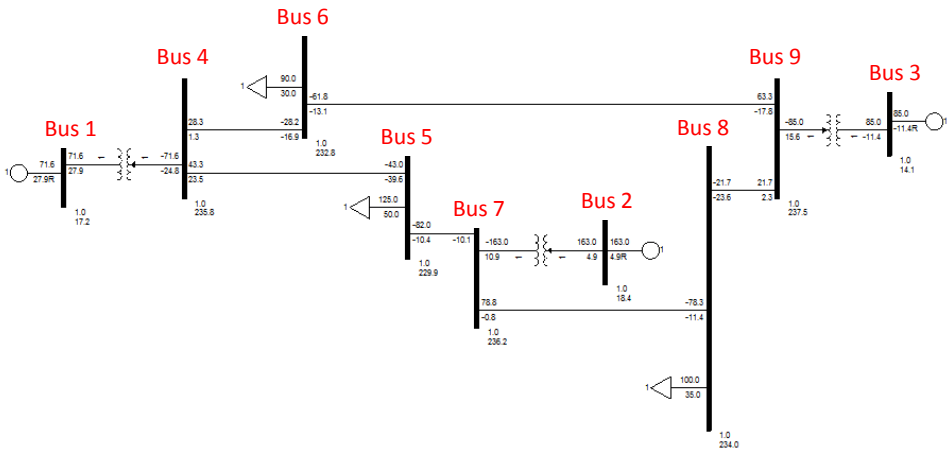

Figure 4.2: IEEE 9 Bus System

4.2 Sensitivity Analysis

The first analysis completed for this thesis using the LE was the relationship between the LE at neighboring buses to PMU buses as a function of current on the line. Our assumption is that the amount of power that is being transferred over the line correlates with the amount of current flowing on the line which will affect the relationship between the two LEs. In order to complete this analysis we ran simulations on the IEEE 9 Bus System using PSSE with complex load models incorporated. Figure 4.2 is a PSSE diagram file, called a slider file, for the IEEE 9 bus system with the bus numbers emphasized.

For the simulations we placed a fault on bus five that cleared without any lines tripping in order to be able to evaluate the LE at that bus. We simulated this fault for the following four scenarios:

1. Low power transfer on the branch from bus 4 to bus 5
   - -13.5 MW at bus 5
   - 24 MVar at bus 5
   - Fault cleared after 5 cycles
2. High power transfer on the branch from bus 4 to bus 5
   - -155.8 MW at bus 5

- -66.8 MVar at bus 5
- Fault cleared after 2.5 cycles

3. Low power transfer on the branch from bus 5 to bus 7
    - -36.8 MW at bus 5
    - -9 MVar at bus 5
    - Fault cleared after 5 cycles
4. High power transfer on the branch from bus 5 to bus 7
    - -119 MW at bus 5
    - -11 MVar at bus 5
    - Fault cleared after 1 cycles

In the above scenarios the negative sign indicates that the power is entering the bus and the positive sign indicates that the power is leaving the bus. The power was adjusted by altering the load and generation of the system to create more power flow along the lines. For the high power cases the solution to the simulation was not converging and therefore the clearing time was reduced until the solution converged. Since current is not an option as an output variable in PSSE the real and reactive power was monitored.

For each of these scenarios we calculated the LE at each bus and plotted the ratio of the neighboring bus to the faulted bus assuming that the faulted bus is where the PMU is located. The voltage at bus five is shown for each scenario in Figure 4.3 and the ratio of the LE between the neighboring bus and faulted bus is shown for each scenario in Figure 4.4.

By visual inspection it looks as if the higher the power transfer, the closer the LE is when compared between the two buses. In both of the high power scenarios the ratio goes above one, where, for both of the low power scenarios the ratio never reaches one. For the high power case between bus five and bus seven there is an unusual drop in the ratio after the first several samples. Since the LE is measuring trajectories based on the difference between two measurements the dynamic oscillation of the signal would make the measurement of the exponent more accurate. Since the voltage is highly damped in the case in which there is high power transfer between bus five and seven the accuracy of the exponent decays with the oscillation. Therefore the ratio between these two exponents after the oscillation decays is less meaningful.

Although these results suggest a relationship between the power on a line and the ratio of the LE between neighboring buses there were no consistent correlations between the ratio min, max or average as a function of the power transfer across the line. Since, the IEEE 9 bus system

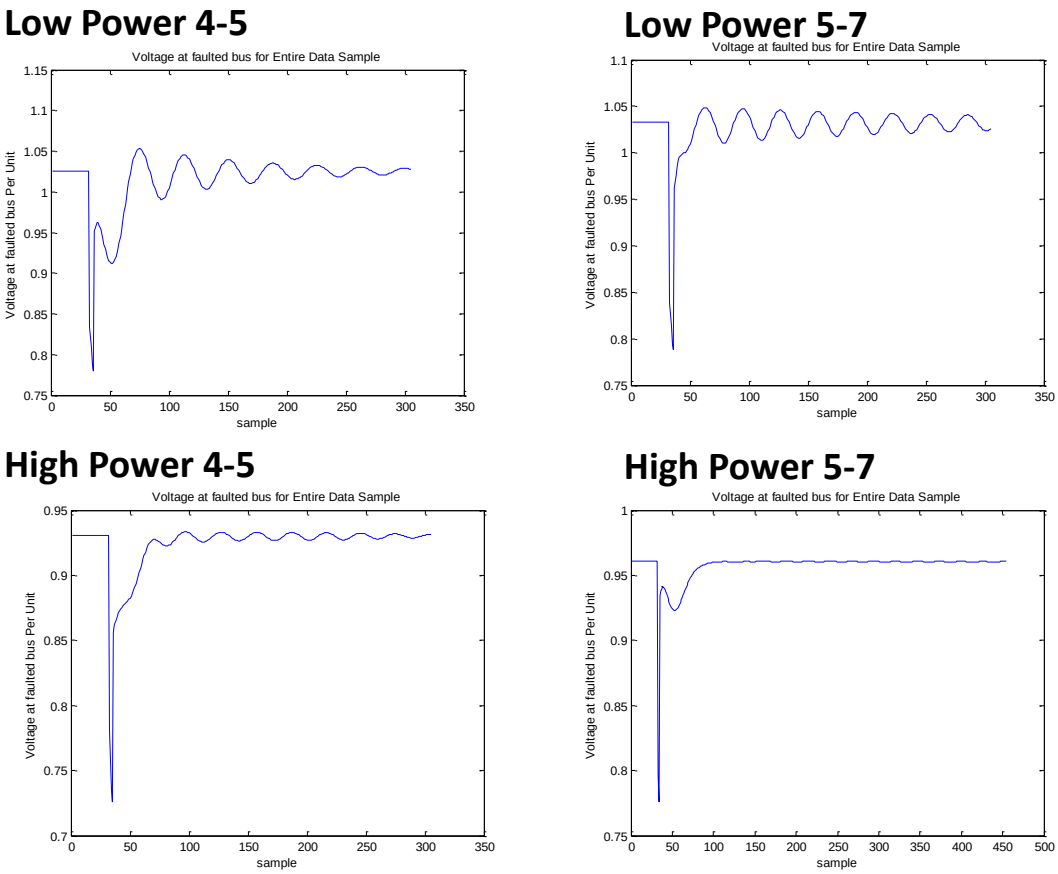

Figure 4.3: Voltage at Bus 5 during Fault Scenario

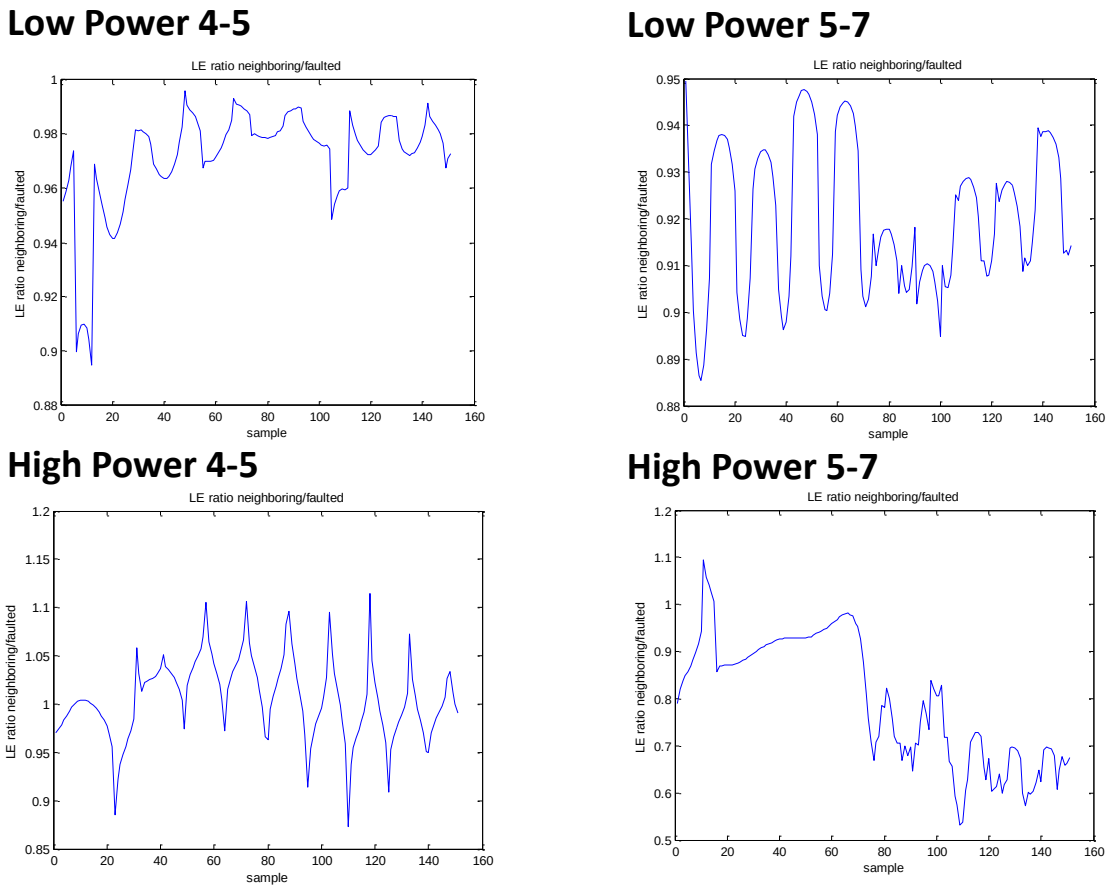

Figure 4.4: LE Ratio of Neighboring Bus over Faulted Bus

is such an unrealistic system given size and inertia, we attempted to verify the results using the IEEE 162 bus system. After completing a similar scenario in the IEEE 162 bus system we were unable to find a correlation between the current or power transfer between two buses and the ratio of the LE.

4.3 Lyapunov Exponent Matrix

The next assessment using the LE for this thesis was creating a matrix of different operating conditions against two metrics of the LE and evaluating the predictive quality of the results. The metrics that are evaluated include the characteristic of the LE plot and the final margin after five seconds of analysis.

The predictive power of a tool is important in power systems because the tool is only useful if it provides time for corrective measures to be taken to avoid an unwanted situation. The main corrective measure to avoid voltage collapse in a critical situation is to shed load. Due to financial and reliability pressures it is undesirable to shed load except in absolute critical situations. Therefore particularly for voltage stability it is desired to have the predictive power of the tool allow ample time for human intervention.

Therefore one of the main goals in this analysis is to evaluate the final margin of the LE after an event where the voltage remains stable. Then compare this to another event occurring after incrementing the load by 400 MW where the voltage collapses. For this situation we hypothesize that the margin will narrow as the system goes towards an unstable load condition when all of the other operating conditions remain the same.

In the analysis for the LE matrix we used four load scenarios, two contingencies and five operating conditions. For each of these 40 combinations the characteristic of the plot of the LE over five seconds and final margin are evaluated.

Load Scenarios:

1. x MW (x = base load)
2. x+400 MW
3. x+1600 MW
4. x+2000 MW

Contingencies:

1. Line Loss (500 kV)

2. Generation Loss (1200 MW)

Table 4.2: Operating Conditions

OC Number	Local Generation Support	SVC	Capacitor Bank	Code
1	OFF (g)	OFF (s)	OFF (c)	gsc
2	OFF (g)	OFF (s)	ON (C)	gsC
3	OFF (g)	ON (S)	OFF (c)	gSc
4	OFF (g)	ON (S)	ON (C)	gSC
5	ON (G)	OFF (s)	OFF (c)	Gsc

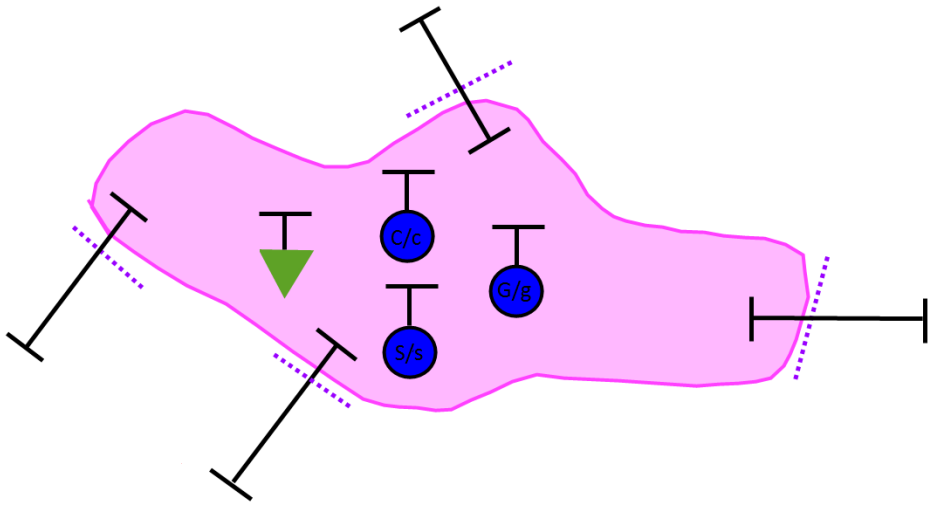

Figure 4.5: Voltage Sensitive Region

Appendix A contains the results of the LE matrix. There are four different tables in which each contains the results for a single contingency across two load scenarios. The results for the generation loss event shown in Figures A.1 and A.2 and the results for the line loss event are shown in Figures A.3 and A.4. All of the scenario combinations that resulted in voltage collapse are highlighted in red. The scenario combination that was stable for one load scenario and collapsed for the next load scenario are highlighted in yellow.

The first two load scenarios surround the load level where the generation loss event caused instability. In particular the scenario with the local generation support off, the SVC on and the capacitor bank off was stable at the load level in the first load scenario but became unstable when 400 MW was added to the system load. Figure 4.6 shows the final LE at five seconds for the 20 scenarios surrounding the generation loss event. Since we are interested in looking at the margin of voltage stable cases we will focus on the results with a negative LE. In all cases the margin of the LE decreases as the load level increases.

The second two load scenarios surround the load level where the line loss event caused instability. In particular the three scenarios with the SVC off was stable at the load level in the third load scenario but became unstable when 400 MW was added to the system load. Figure 4.7 shows the final LE at five seconds for the 20 scenarios surrounding the line loss event. Since we are interested in looking at the margin of voltage stable cases we will focus on the results with a negative LE. In all cases the margin of the LE decreases as the load level increases.

Some additional observations surround the characteristic of the LE, the event type and the local voltage support type. First there is a definite difference in the characteristic of the LE for the voltage collapse cases versus the cases that remained voltage stable. The initial oscillation has a smooth transition at its first minimum point for the voltage collapse cases whereas the ones that remain stable have a sharp transition at the first minimum. For the cases that resulted in voltage collapse the first minimum occurred within two seconds where as for stalbe cases the first minimum occurred within one second. Also the system remained voltage stable at a higher load level for the line loss event than the generation loss event. Finally the difference between the capacitor bank being on or off had much less effect on voltage stability than the status of the SVC being on or off.

The final margin of the LE shows potential for both relative and absolute predictability. Since the margin decreases as the load increases to a point where the next contingency results in voltage collapse, it may provide information about the proximity of the system to instability. In all cases the final margin at the five second correctly indicated the stability of the system. This may mean that the LE may always be able to indicate if a system remained stable or if a system collapses as long as the final margin is evaluated after a certain amount of time. For stable cases the last sign change occurred by 3.11 seconds and for unstable cases the last sign change occurred around the 5 second mark. The difference in the characteristic of the LE was

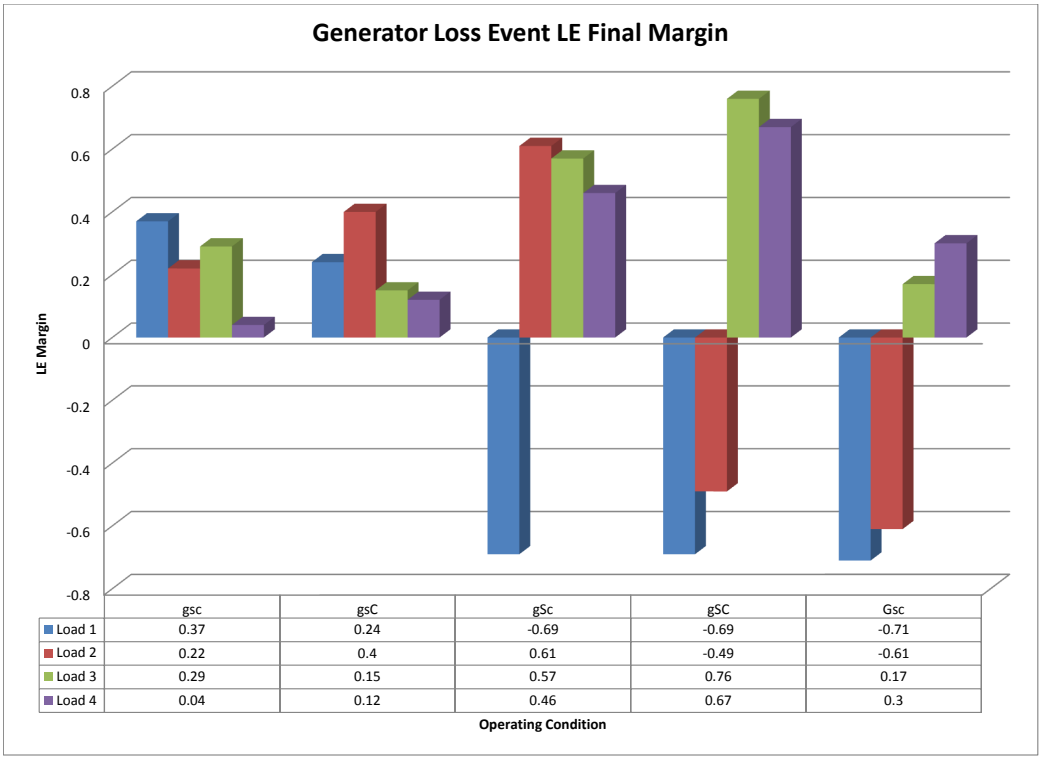

	gsc	gsC	gSc	gSC	Gsc
Load 1	0.37	0.24	-0.69	-0.69	-0.71
Load 2	0.22	0.4	0.61	-0.49	-0.61
Load 3	0.29	0.15	0.57	0.76	0.17
Load 4	0.04	0.12	0.46	0.67	0.3

Figure 4.6: Final Margin Generation Loss Event

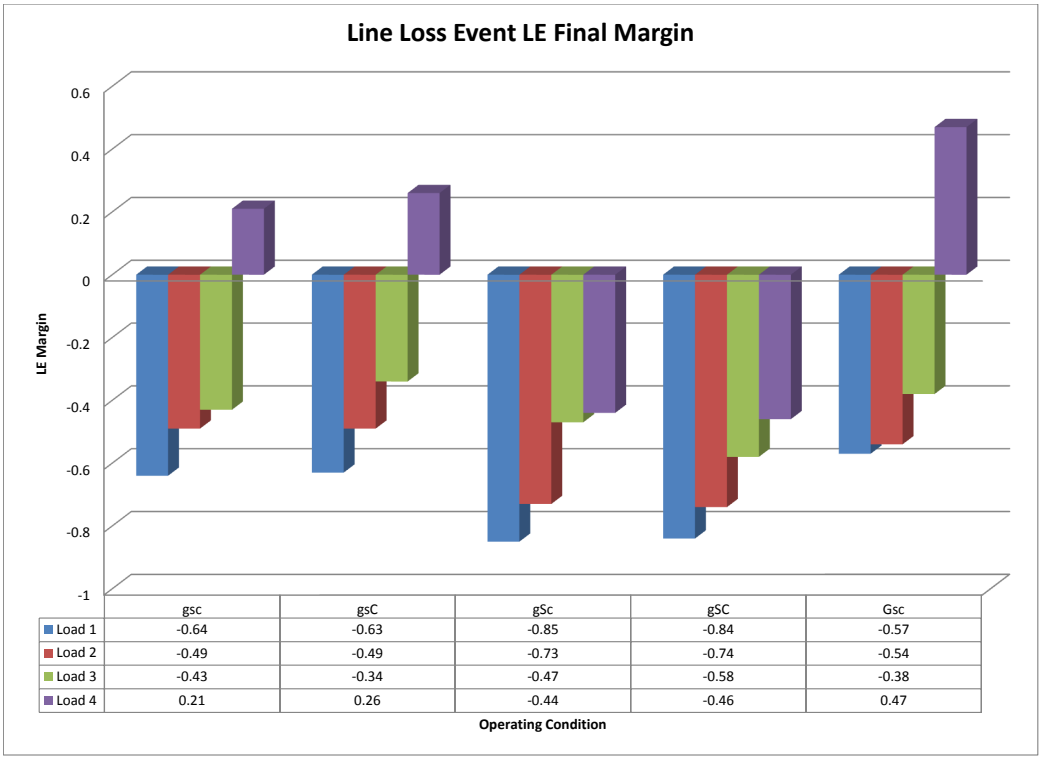

	gsc	gsC	gSc	gSC	Gsc
Load 1	-0.64	-0.63	-0.85	-0.84	-0.57
Load 2	-0.49	-0.49	-0.73	-0.74	-0.54
Load 3	-0.43	-0.34	-0.47	-0.58	-0.38
Load 4	0.21	0.26	-0.44	-0.46	0.47

Figure 4.7: Final Margin Line Loss Event

also apparent between the voltage stable and voltage collapse cases. However, both the sign and plot characteristic indicators happen during the event without time for human intervention.

The final margin of the LE shows potential for relative predictability. The final margin in all of the scenarios decreased before the load reached a level where the contingency caused voltage collapse. Therefore, these results indicate that the LE may be a good predictor of how close a system is to voltage collapse.

Chapter 5

Voltage Stability Assessment Using The Decision Tree

The implementation of PMUs has created a large amount of data for analysis. This opens opportunities for using techniques applied to big data such as data mining. One of these techniques is known as decision trees or classification trees. This technique uses a large set of data in which the desired target to be predicted is identified and finds commonalities surrounding the target. Ultimately it takes the information with the most predictive value around the target and creates rules. These rules can be applied to future data in real-time in order to predict a certain outcome.

For this particular study we are interested in predicting short-term voltage stability by using PMU data in real-time. Since data for voltage collapse from the real system is nonexistent the data used to build the decision tree must come from simulations on the system model. For our evaluation we used Duke Energy's system model and other PSSE files that were used for a Summer 2014 voltage study conducted by system planning.

5.1 Simulations

In order to create a set of big data that would resemble the data seen by the PMUs on the system we had to create a channel file in PSSE that would give us the same values that are obtained or calculated by the PMUs. A channel file specifies the measurements that PSSE should monitor during the simulations. Therefore, before running the simulations we identified the buses and lines where the PMUs are located in the voltage sensitive region of study. Next, we created a channel file that captured the bus voltage magnitude and angle, bus frequency and real and reactive power on the line. When the latter two are specified in PSSE it captures the quantities entering (negative) and exiting (positive) each bus at the end of the branch. This

is the same convention that is used for the PMUs. For each of these we used the same name for the quantity as the tag name used on the PMUs for easy comparison. Current magnitude and angle is not a specified output in PSSE. However, this can be calculated using the other values if it is desired to find the current instead of the power. Likewise the values of real and reactive power can be calculated at the PMU using the measured quantities of current.

Another difference between the PMU data from the real system and the PSSE simulated data is the presence of the three phases. PSSE models the system as a single phase equivalent model and therefore assumes that the system is balanced between phases which is pretty accurate when considering the transmission system where the PMUs are placed. Therefore, we use the positive sequence values from the PMU to compare to the rules we create with the decision tree.

After creating this channel file we incorporated it in the files used to create simulations for the Summer 2014 voltage study. These simulation files included base case files that represented different operating conditions, PSSE response files that would automatically scale load and re-dispatch generation and files that would simulate different contingencies such as the loss of a generator or the loss of a line.

There are a few important things to point out about these simulation files. For the portion that would scale the load, the load was divided among residential, commercial and industrial in which the residential and commercial load is scaled and the industrial load remains constant. This is more representative of how the load fluctuates in the real system. Also, as load increases in a PSSE case there has to be generation created to match the load. If this is not specified it comes from the slack bus generator. When this is the case it is important to make sure the power supplied by the slack bus generator is realistic. However, in our study the generator dispatch to match the load is specified by a file included in the program. This file dispatches the generation economically and when the load increases beyond the capacity of the subsystem the power is imported from other neighboring utilities in a realistic pattern.

Another important thing to understand is that the simulations are based on a model of the system which in some ways can react differently than the real system. Normally the differences are small enough that many planning an operating decisions can be made by leaving some margin of error. In doing these simulations for the LE and decision tree we did not incorporate a margin of error. This may be desirable to add for actual implementation. In addition to the fact that the simulations are based on a model, they are also based on a set of assumptions as far as the participation factors of the load scaling and the pattern of dispatching generation and importing power. If either one of these is different than specified in the simulation the power will flow differently through the system which may affect the outcome. Also the market of power sometimes can dictate which generators are supplying power to meet certain loads. These factors were considered and intelligent decisions were made when system planning created

these simulation files.

For an initial test run with the decision tree we completed 276 simulations. Of these 81 were voltage collapse cases, 195 were voltage stable cases, 140 were with a generation loss event, 136 were with a line loss event, 72/204 were with the SVC on/off and 102/174 were with the capacitor bank on/off. To create these we chose a set of operating conditions that were sensitive to voltage collapse in which there was less local generation. We created dynamic simulations for a line loss contingency and a generation loss contingency at several load levels around the point in which the contingency would cause voltage collapse. For all of these simulations the output file that contained the information from the location of the area PMUs were split between those in which the voltage recovered (voltage stable) and those in which the voltage did not recover (voltage collapse).

When we ran the data through the decision tree algorithm it was overwhelmed by the difference between the contingencies with little other information. Therefore the data was split between the generation loss event and the line loss event to create two decision trees. With less than 200 cases there was only enough data to build the decision tree. When enough data is present it is customary to split the data into three sets, one for building the decision tree, one for validating the different models produced and the one to test the decision tree for accuracy.

After getting some promising results from this initial data we decided to run enough simulations to both build and test the decision tree. We did this by decreasing the incremental load increase, increasing the number of iterations (range of the load), focusing on the generation loss contingency and then running the simulation on more operating conditions. For this single contingency we ran 3,128 additional simulations.

This research effort is meant to test the possible usefulness of different tools. If results are promising, the idea would be to automate a process to create a few thousand simulations per contingency at several different operating conditions and load levels to create a decision tree for each contingency. Once the decision trees are built the PMU data could be checked against the decision trees in real-time and if the conditions are met for voltage collapse given a specific contingency this information can be relayed to the operator before any contingency occurs. For example an alert may be in the form of "vulnerable to voltage collapse for the loss of generating unit B."

5.2 Decision Tree

5.2.1 Preliminary Decision Tree

With the help from our collaborators at SAS we converted the simulation files to data files that could be read by SAS Enterprise Miner, a software package from SAS that specializes in

different data mining techniques including the decision tree. In the conversion process PMU pairs were created by their location in order to have a common reference for the phase angles between the simulation data and the PMU data. Since the decision tree only uses static data a single timestamp of data from all of the PMU tags was copied from each simulation to a single data file. So that a prediction based on this data could warn system operators when the system is at a certain state prior to the contingency causing voltage collapse the timestamp was chosen before the contingency occurred in the simulation. After realizing that it was better to isolate each contingency, we split the simulations into two data files, one per contingency. The data that we used to create the results below came from the 140 cases for the generation loss contingency.

The SAS Enterprise Miner decision tree algorithm produced the results shown in Figure 5.1. This decision tree created three rules. The first node in the decision tree represents the complete set of data that was evaluated. The number of cases that are evaluated by this node are all 140 cases. Of the 140 cases 50.71 percent resulted in voltage collapse and 49.29 percent resulted in voltage recovery.

The branches that come out of the node define the first rule and split the data based on the rule. The first rule looks at the reactive power, MVars, of a 230kV bus in the systems voltage sensitive region. It splits the data between cases in which this bus had less than 52.7544 MVar entering the bus and cases that had 52.7544 MVar or more entering the bus. The second layer of nodes contain information about the cases that were spilt by the first rule. The node on the right contains the information about the cases in which the reactive power entering the 230 kV bus was equal to or greater than 52.7544 MVar. There were 54 cases that satisfied this condition. Of the 54 cases 1.85 percent resulted in voltage collapse and 98.15 percent resulted in voltage recovery. The node on the left contains information about the cases in which the reactive power entering the 230 kV bus was less than 52.7544 MVars. There were 86 cases that satisfied this condition. Of the 86 cases 81.40 percent resulted in voltage collapse and 18.60 percent resulted in voltage recovery.

The second rule is defined by the branches that come out of the second layer node that has a higher number of voltage collapse cases. The most significant indicator of stability in this subset of data was whether the SVC is on or off and therefore is set as the second rule. The third layer node on the right contains the information about the cases in which the SVC is off. There were 54 cases that satisfied this condition. Of the 54 cases 92.59 percent resulted in voltage collapse and 7.41 percent resulted in voltage recovery. The third layer node on the left contains information about the cases in which the SVC is on. There were 32 cases that satisfied this condition. Of the 32 cases 62.50 percent resulted in voltage collapse and 37.50 percent resulted in voltage recovery.

The third rule specifies the condition that may cause voltage collapse even when the SVC is

in service. Here it is important to note that there are sometimes multiple rules that have an equal level of predictability. The decision tree algorithm selects one automatically. However, there is an interactive mode in the program that lists other rules and their level of predictability. In this case there were a few rules that had an equal value of predictability. The original rule divided the data by the phase angle difference between two PMUs being greater than a certain degree. Since the original rule would create a need for the calculation of PMU data before processing we decided to use a rule that had an equal level of predictability but wouldn't require any calculation. For this purpose we chose to use the voltage magnitude at one of the 500 kV buses in the systems voltage sensitive region. This rule divides the data between cases in which the voltage magnitude is less than 1.0471 per unit and cases in which the voltage magnitude is equal to or greater than 1.0471 per unit. Although the actual system voltage at the 500 kV buses is 525 kV the base for purposes of converting to a per unit quantity is 500 kV. Therefore, if the voltage is 525 kV the per unit voltage is 1.05. The fourth level node on the right contains the information about the cases in which the voltage magnitude is equal to or greater than 1.0471 per unit. There were 12 cases that satisfied this condition. Of the 12 cases 100 percent resulted in voltage recovery. The child node on the left contains information about the cases in which the voltage magnitude is less than 1.0471 per unit. There were 20 cases that satisfied this condition. Of the 20 cases 100 percent resulted in voltage collapse.

Since, most of the time the SVC is in service we focused on the times in which the SVC was in service and the generation loss contingency still caused voltage collapse. In other words we want to focus on the bottom left node in which all of the cases resulted in voltage collapse. The three rules that apply to this data include the following:

1. 230 kV bus MVar $<$ -52.7544
2. SVC is on
3. 500 kV bus Vmag $<$ 1.0471 per unit

Assuming the SVC is on we can search the PMU data for any instance in which the reactive power entering the 230 kV bus is less than 52.7544 MVar and the voltage magnitude at the 500 kV bus is less than 1.0471 per unit or 523.55 kV. Since the convention of the PMU data matches the simulation data where the power or current entering a bus is negative and power or current exiting a bus is positive we can search the data for values less than -52.7544 MVar. Upon searching the PMU data that we have obtained since the beginning of the year there was only one case in which there would have been a momentary alarm in which both of these conditions were true shown in Figure 5.2. This condition was only present for two PMU timestamps or 0.067 seconds. The alarm would indicate that the area is vulnerable to voltage collapse if the generation loss event studied occurs.

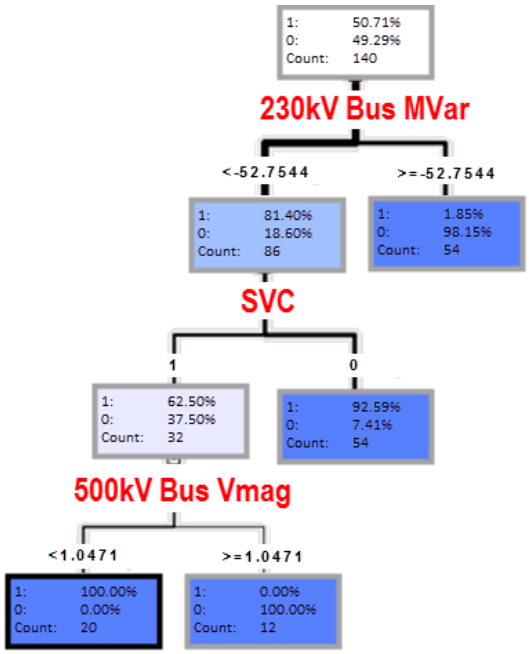

Figure 5.1: Preliminary Decision Tree

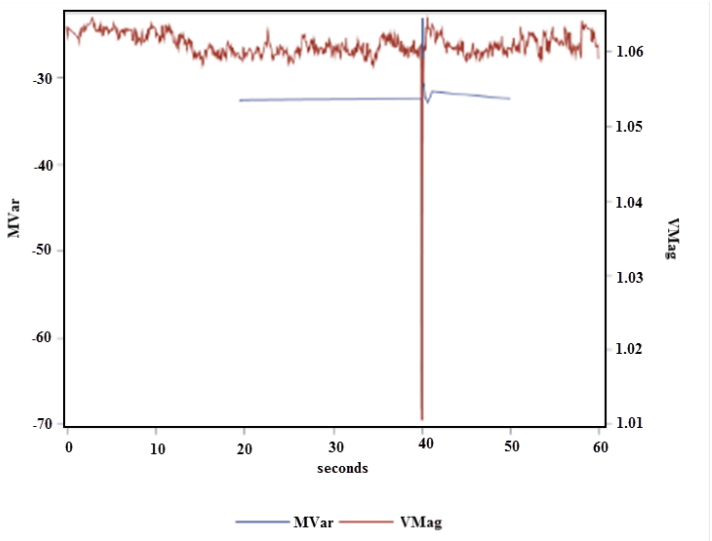

Figure 5.2: PMU Data for Decision Tree Rules Momentary Alarm

5.2.2 Final Decision Tree

With the help from our collaborators at SAS we converted the larger set of simulation files for the generation loss contingency to data files that could be read by SAS Enterprise Miner. Since there was enough data we partitioned the data into three categories; 1251 cases for training the decision tree, 937 cases for validation, and 940 to test the decision tree. The training data set is used to find partitions and create a family of models. The validation data is used to make estimates and select one model from the family of models produced by the training data. The testing data set is used to evaluate the resulting decision tree [67]. The SAS Enterprise Miner decision tree algorithm produced the results shown in Figure 5.3. This decision tree created three combinations of rules that lead to collapse 100 percent of the time in the training data.

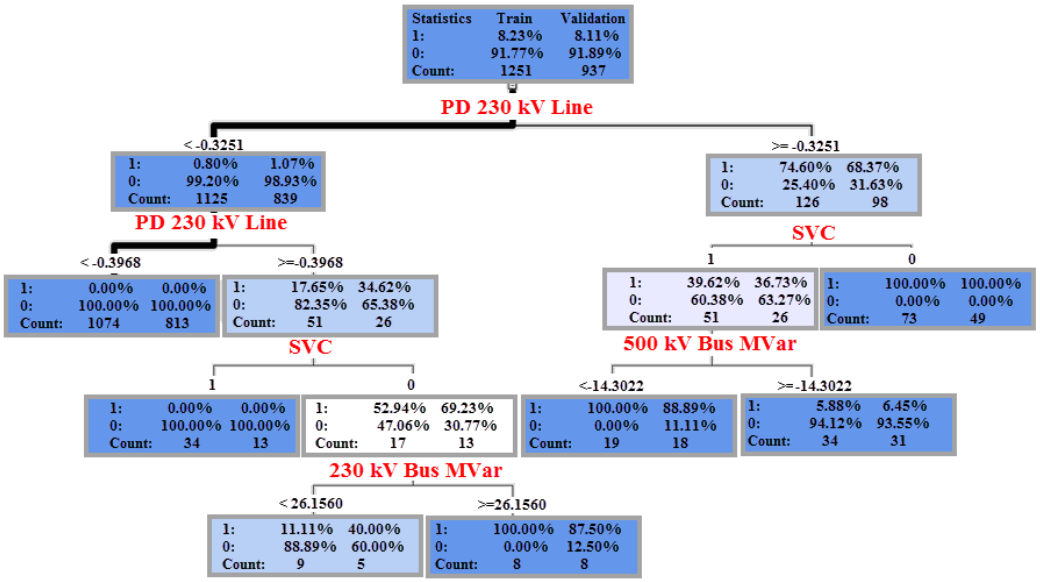

Figure 5.3: Final Decision Tree

Since, most of the time the SVC is in service we focused on the times in which the SVC was in service and the generation loss contingency still caused voltage collapse. The three rules that apply to this node include the following:

1. 230 kV line PD (voltage phase angle difference) < -0.3251 degrees
2. SVC is on
3. 500 kV bus MVars < -14.3022 MVars

Assuming the SVC is on we can search the PMU data for any instance in which the voltage phase difference between the two 230 kV buses specified by the rule is less than -0.3251 degrees and the reactive power entering the 500 kV bus is greater than 14.3022 MVars.

After building the decision tree, SAS Enterprise Miner completes some statistical scoring of the decision tree. The event classification table gives the number of false negatives and false positives in both the training data set and validation data set. For the training data set there were 3 false negatives meaning that the rules created by the decision tree failed to correctly predict when the system was vunerable to a voltage collapse incident 3 out of 1,251 times. For the validation data there were three false negatives and 4 false positives. This means that the decision tree rules failed to predict the vulnerability to voltage collapse 3 out of 937 times and falsely predicted vulnerability to voltage collapse 4 out of 937 times. The false positives and false negatives directly relate to the misclassification rate in the fit statistics shown in Table 5.2. If you take the number of false positives and false negatives and divide by the total number of data in each data set the result is considered the misclassification rate. For the training data the misclassification rate is 0.002398 and for the validation data the misclassification rate is 0.007471. Table 5.2 shows these rounded to the second decimal place. The accuracy of the decision tree can be determined by subtracting the misclassification rate from one and multiplying by 100 percent. Therefore all of the data sets had over 99 percent accuracy.

Table 5.1: Event Classification Table

Data Role	False Negative	True Negative	False Positive	True Positive
Train Target	3	1148	0	100
Validate Target	3	857	4	73

Table 5.2: Fit Statistics

Fit Statistics	Train	Validation	Test
Sum of Frequencies	1251	937	940
Misclassification Rate	0	0.01	0.01
Maximum Absolute Error	0.94	1.00	1.00
Sum of Squared Errors	5.54	13.20	9.19
Average Squared Error	0.00	0.01	0.00
Root Average Squared Error	0.05	0.08	0.07
Divisor for ASE	2502	1874	1880
Total Degrees of Freedom	1250	.	.

5.3 PV Curve Analysis

Since we used specific operating conditions and contingencies for both the LE matrix and the decision tree we wanted to evaluate the maximum power transfer across a given corridor using the classical PV curve. In addition we wanted to evaluate another critical line loss in order to determine the sensitivity of the line that was studied. For the different contingencies our analysis included the steady state before and after the line loss or generator loss. The corridor evaluated was from a 500 kV bus to a 230 kV bus in the voltage sensitive area. In order to determine the power transfer limit across the corridor we needed the equivalent impedance between the two buses. The PSSE simulation model that we used incorporates the whole eastern interconnection. In small systems the impedance matrix is easy to construct and provides information regarding the equivalent impedance between two buses. However, with such a large system it is unrealistic to construct an impedance matrix by hand. Therefore, we requested the value from Protection and Controls Engineering. They use Aspen OneLiner a software that has a built in short circuit program that can easily find available fault current and symmetrical component impedance values. We requested the equivalent impedance for the following five scenarios and evaluated each scenario for the case where the load is at unity power factor and for the case where the load is at 0.5 power factor.

Table 5.3: Operating Condition Cases and Equivalent Impedance of Corridor

Case	Description	R	X
C0	All lines in service, all generation on	0.0035	0.0409
C1	All lines in service, one local generating unit off	0.0032	0.0393
C2	All lines in service, two local generating units off	0.0029	0.0373
C3	500 kV line out of service, one local generating unit off	0.0176	0.1399
C4	Two 230 kV lines out of service, one local generating unit off	0.0042	0.0457

For the analysis we used an equation derived in [59] from the load flow equations. Given the power factor of the load below:

$$pf = \cos\theta_D \tag{5.1}$$

The ratio of reactive power over real power can be expressed as follows:

$$\frac{Q_D}{P_D} = \tan\theta_D = \beta \tag{5.2}$$

Incorporating this into the load flow equations we can form the following equation and use this to plot the PV curve:

$$|V_2|^2 = \frac{|Y_{line}|^2|V_1|^2 - 2P_D(G_{line} - \beta B_{line})}{2|Y_{line}|^2}$$

$$\pm\sqrt{\frac{[2P_D(G_{line} - \beta B_{line}) - |Y_{line}|^2|V_1|^2]^2 - 4|Y_{line}|^2P_D^2(1+\beta^2)}{2|Y_{line}|^2}} \tag{5.3}$$

From this we can calculate the maximum power transfer (5.4) and the critical voltage (5.5).

$$[2P_{D_{cr}}(G_{line} - \beta B_{line}) - |Y_{line}|^2|V_1|^2]^2 - 4|Y_{line}|^2P_{D_{cr}}^2(1+\beta^2) = 0 \tag{5.4}$$

$$|V_{2_{cr}}|^2 = \frac{|Y_{line}|^2|V_1|^2 - 2P_{D_{cr}}(G_{line} - \beta B_{line})}{2|Y_{line}|^2} \tag{5.5}$$

The results show that the voltage stability of the selected transmission corridor and load bus is most affected by the 500 kV line loss event that was studied throughout the analysis. For this case the maximum power transfer for a unity power factor load is 14.37 MW and for a load with a power factor of 0.5 was 10.31 MW. The two 230 kV lines had the second lowest maximum power transfer at 59.9 MW for a unity power factor load and 42.135 MW for a load with a 0.5 power factor. However the maximum power transfer for this particular corridor increases with less generation. With all of the generation on, the maximum power transfer is 71.82 MW with a unity power factor and 50.33 MW with 0.5 power factor shown by the red curve. With two units off the maximum power is 86.6 MW with a unity power factor and 60.41 with 0.5 power factor shown by the cyan curve. The decrease in maximum power with the loss of one generating unit was between 8.3 to 9.3 percent.

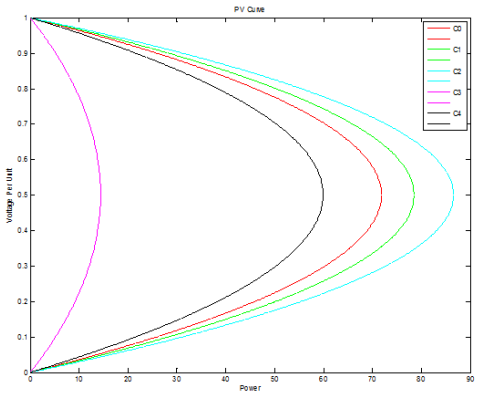

Figure 5.4: PV Curve Unity Power Factor

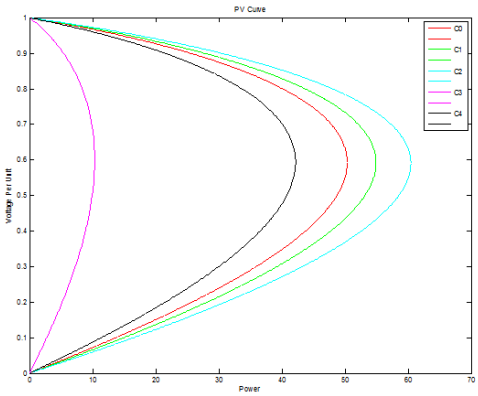

Figure 5.5: PV Curve 0.5 Power Factor

As expected the maximum power transfer to a load with a power factor of 0.5 was much less than that for the case of unity power factor. This difference ranged from 28.2 to 30.2 percent. The critical voltage in the scenario with the smaller power factor was significantly larger than the case for unity power factor. This difference was between 15.3 to 16.5 percent. In all cases the power transfer decreased and the critical voltage increased as the resistance and reactance increased.

Figure 5.6: Maximum Power Transfer

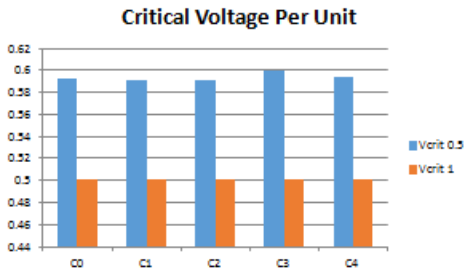

Figure 5.7: Critical Voltage

Table 5.4: PV Curve Summary

Case	Power Factor	Resistance	Reactance	Max Power	Critical V
C0	1	0.0035	0.0409	71.8204	0.5005
C0	0.5	0.0035	0.0409	50.3318	0.5925
C1	1	0.0032	0.0393	78.513	0.5004
C1	0.5	0.0032	0.0393	54.8879	0.5917
C2	1	0.0029	0.0373	86.5973	0.5004
C2	0.5	0.0029	0.0373	60.4087	0.591
C3	1	0.0176	0.1399	14.3727	0.501
C3	0.5	0.0176	0.1399	10.3145	0.6002
C4	1	0.0042	0.0457	59.9003	0.5005
C4	0.5	0.0042	0.0457	42.135	0.5937

When looking at the steady state analysis of voltage stability between scenarios in comparison with the dynamic results there are significant differences. In the steady state analysis the line loss events were more voltage sensitive than the generation loss events. Also, voltage stability increases with the number of generating units on in the dynamic analysis where the opposite is true for the steady state analysis. The steady state results given the corridor method

of voltage stability assessment are highly dependent on the choice of the corridor. In this case the corridor source bus is on the opposite side of the sink bus than the generating units. The line loss event that was most significant was in the path of the corridor. Therefore if we chose a source bus for the corridor on the same side as the generating units or a line loss that was not in the path of the corridor the results could differ significantly. Although these results didn't line up with the sensitivities expected given the experience with my dynamic simulations, this could be due to the selection of the corridor and the location of lines and generating units.

Chapter 6

Conclusion and Future Work

There has been increasing penetration of PMUs in the United States due to smart grid initiatives. Duke Energy has installed 125 PMUs across a portion of its territory and has provided this data for research by a team with members from Duke Energy, SAS and NCSU. The baselining research covered in this paper includes baselining ranges of values surrounding events and dynamic baselining. The focus of the PMU application research was the assessment of short-term voltage stability using a mathematical based approach, the LE, and a statistical data mining based approach, the decision tree.

6.1 Baselining

The first method of baselining focuses on finding the range of values of certain measurements seen by the PMUs over different events. For all measurements the PMU data showed a larger response the closer the event was to the PMU and when the event occurred at the same voltage level as the PMU. All of the voltage phase angle differences were minimal. This may be due to the timing of the events being during the Fall season when much less power is produced and consumed. Some of the PMU pairs had similar angle differences across all of the events, where some of the PMU pairs had very different angle differences across the events. This could be a trend that some of the lines in the former case have a more consistent power flow than those in the latter case. In all but one PMU pair over one event the sign of the angle difference remained the same before and after each event indicating that the power continued to flow in the same direction.

The standard deviation of the average values for voltage phase angle difference was much larger than the standard deviation of the average values of voltage magnitude and frequency. This is likely due to the fact that frequency and voltage are highly monitored and controlled in power systems. Voltage phase angle difference across lines is a function of the real power

transfer which varies throughout the day and seasons. All of these results were within expected limits.

Dynamic baselining around events was the second form of baselining that we did using the PMU data. The range of slow modes across all PMUs over four events was 0.4902 Hz to 0.8914 Hz with an average of 0.7431 Hz and a standard deviation of 0.1127. The median was 0.7230 Hz and the most common values when rounded to the 2nd decimal place, each occurring three times was 0.63 Hz and 0.87 Hz. The damping ranged from 0.1575 to 0.8051 with an average of 0.3355 and a standard deviation of 0.1451. We were unable to find any consistent inter-area modes of oscillation. For the most part the post event oscillations were well damped and difficult to evaluate. The difficulty in extracting inter-area modes could be due to the fact that the system under study is a highly meshed system, densely connected generation and load, where inter-area modes are more significant when there are long transmission corridors between generation and load pockets.

6.2 Voltage Stability

Voltage stability has become an increasing concern for most large power systems. Our goal is to find an application for the PMU data in the assessment of short-term voltage stability with a specific effort towards a predictive method, preferably one contingency in advance (N-1) scenario. With combined effort from NCSU and SAS, we explored using the LE and the decision tree as a tool for the assessment of voltage stability.

First, we tested the ratio of the LE between neighboring buses as a function of current on the line. The goal of this analysis being the ability to expand the visibility of voltage stability to a bus neighboring a bus monitored by a PMU. Although there were promising results when testing the method on the IEEE 9 bus system, we were not able to get consistent results when using the IEEE 162 bus system.

Next we wanted to evaluate the characteristic of the LE as well as its final margin as a function of operating conditions, contingencies and proximity to instability. From our analysis we found the sign of the exponent to correctly indicate stability after five seconds of evaluation. The last sign change occurred by 3.11 seconds for the stable cases. Also, there was a definite difference in the characteristic of the LE in a voltage stable case versus a voltage collapse case which was notable at the first minimum. For stable cases this occurred within the first second and for voltage collapse cases this occurred within the first two seconds. Both of these appear to be good indicators of a voltage collapse as it is occurring. However, short-term voltage instability can cause collapse in just a few seconds leaving little or no time to act with these predictors.

Our hypothesis was that the final margin of the LE would decrease as the system became more stressed, defined by an increased load level to a point where a given contingency would

cause voltage collapse. In all cases the final margin at five seconds decreased as the load level increased. One additional observation with this is that the margin fluctuates with the characteristic of the LE. Therefore a more accurate assessment of the final margin may be to evaluate a local maxima during a certain time period. In conclusion the LE is a good predictor during an event that causes voltage collapse and shows potential for relative predictability or predicting how close a region is to instability by assessing the final margin.

The decision tree is a data mining technique that uses tools from both the statistical and cognitive types of data mining. In our analysis we used SAS Enterprise Miner to build a decision tree focused on a single contingency with our initial set of simulation data which included 140 simulations for a generation loss event. Since this was not enough data to partition for testing purposes we ran additional simulations with more granularity focused on the generation loss event in order to build a decision tree that we could evaluate. To create this data we increased the load range, decreased the load increment and increased the number of operating conditions to produce 3,128 cases.

Since the status of the SVC plays an important role in the voltage stability of the voltage sensitive region and it is normally in service we focused on the rules in which the SVC is in service and the generation loss contingency still resulted in voltage collapse. The initial decision tree rules included the reactive power entering a 230 kV bus being greater than 52.75 MVars and the voltage magnitude at a 500 kV bus being less then 1.047 per unit. When searching through archived PMU data there was only one instance that the data matched these rules momentarily. The final decision tree rules included the voltage phase angle difference between two 230 kV buses being greater than -0.3251 degrees and the reactive power entering a 500 kV bus being greater than 14.3022 MVars.

Since we had enough data to partition and test our final decision tree we were able to evaluate its accuracy. There were three sets of data evaluated; training data set, validation data set, testing data set. For all three data sets the accuracy was over 99 percent corresponding to a misclassification rate of lest than 0.01. These are promising results for the prediction of vulnerability to voltage collapse given the specific generation loss contingency evaluated. An additional benefit to this method is that it provides information about specific conditions, decision tree rules, that have caused the alarm and the contingency that would result in voltage collapse. With this information an operator would have knowledge of the critical contingency as well as be able to focus on a single rule to avoid the vulnerable situation.

Some other benefits to the decision tree other than the predictability for an (N-1) situation, include the fact that after the initial set up it would be easy to automate creating simulations and building the decision tree. The rules are easy to interpret and incorporate into current monitoring systems. The alarm would be actionable with information of a critical contingency. One negative aspect of this tool is the fact that it would be impossible to run simulations on

every possible scenario so it would not be all inclusive. However, most voltage studies done currently only assess certain situations that system planners and operators, with knowledge of the system, think are critical. If this knowledge was incorporated into the process it may be exhaustive enough. Another downfall of this method is that as all statistical methods the prediction is never absolute. Ultimately, given the difficult task of detecting short-term voltage instability, an alert in this form may be beneficial to incorporate into operations since the testing process shows over 99 percent accuracy.

6.3 Future Work

As time progresses there will be more PMU data for events archived. For future baselining work, getting a larger sample of event data to evaluate would provide a more realistic range and average as well as provide opportunities to divide the data between seasons and time of day. To allow for this type of analysis getting events during both daily peak hours and non peak hours over all four seasons Fall, Winter, Summer and Spring would be ideal. Some other ways to expand the input to this baselining technique would include exploring different transmission voltages, event types and other measurements such as current and power.

Dynamic baselining using a system identification method such as ERA requires that the input to the system be significant enough for the dynamics of the system to be present in the output. For power systems this would be the severity of the fault or disturbance. This type of analysis would also benefit from having archived event data. For dynamic baselining it is important that the data quality is good and there are no missing values. Once the data quality issues are resolved more data will be able to be used in this process. If there is a larger sample of data that can be evaluated, we may be able to better extract the modal content of the system.

For thoroughly representative event baselining the development of a consistent, automatic technique that would detect and evaluate event data in real-time would be ideal. A combination of techniques developed by SAS and NCSU over this project could be used to accomplish this. SAS has developed an algorithm to detect events and possibly determine the type of event from the time series data. Once detected and categorized the range of values and dynamic analysis could be performed and statistical baselining data could be updated.

Future work in the assessment of short-term voltage stability using the LE would be to evaluate the final margin at the last local maxima for more accuracy. In addition, a sample of simulation data that has more granularity as far as load increment and operating conditions may provide better estimate of a consistent margin in which the next contingency would result in voltage collapse. The possible dependence of this margin with respect to the contingency that causes voltage collapse may be interesting to evaluate. The sign of the LE after five seconds or the evaluation first minimum of the plot characteristic may be useful in the assessment of

long-term voltage stability. From Table 3.1 most of the voltage collapse events had a longer time frame than is typical for short-term voltage stability.

Future work involving the decision tree would include scanning the archived PMU data for data that matches the rules created by the final decision tree in order to further validate the realistic nature of the rules created. Also, using the contingencies and operating conditions from the system voltage study to create an automated process to produce simulation data and build a set of decision trees for each critical contingency. Once these are built the PMU data can be scanned for incidences that match the decision tree rules in real-time. This could be incorporated outside of the control room initially to make sure that the rules do not produce too many false positive alarms that would deter acceptance, add an element of needless distraction and become ineffective in the case of a true positive.

REFERENCES

[1] M. Glavic, D. Novosel, E. Heredia, D. Kosterev, A. Salazar, F. Habibi-Ashrafi, and M. Donnelly, "See it fast to keep calm," *IEEE Power and Energy Magazine*, vol. 10, no. 4, p. 43, 2012.

[2] M. Vutsinas, "Phasor measurement units." Lunch and Learn, 2013.

[3] A. Chakrabortty and P. P. Khargonekar, "Introduction to wide-area control of power systems," in *American Control Conference (ACC), 2013*, pp. 6758–6770, IEEE, 2013.

[4] A. G. Phadke, "Synchronized phasor measurements-a historical overview," in *Transmission and Distribution Conference and Exhibition 2002: Asia Pacific. IEEE/PES*, vol. 1, pp. 476–479, IEEE, 2002.

[5] A. G. Phadke and J. S. Thorp, *Synchronized phasor measurements and their applications*. Springer, 2008.

[6] X. Mou, W. Li, and Z. Li, "Pmu placement for voltage stability assessment and monitoring of power systems," in *Power Electronics and Motion Control Conference (IPEMC), 2012 7th International*, vol. 2, pp. 1488–1491, IEEE, 2012.

[7] A. Silverstein and J. E. Dagle, "Successes and challenges for synchrophasor technology: An update from the north american synchrophasor initiative," in *System Science (HICSS), 2012 45th Hawaii International Conference on*, pp. 2091–2095, IEEE, 2012.

[8] A. Kaci, I. Kamwa, L.-A. Dessaint, and S. Guillon, "Synchrophasor data baselining and mining for online monitoring of dynamic security limits,"

[9] H. Zhao, "A new state estimation model of utilizing pmu measurements," in *Power System Technology, 2006. PowerCon 2006. International Conference on*, pp. 1–5, IEEE, 2006.

[10] R. Avila-Rosales, M. Rice, J. Giri, L. Beard, and F. Galvan, "Recent experience with a hybrid scada/pmu on-line state estimator," in *Power & Energy Society General Meeting, 2009. PES'09. IEEE*, pp. 1–8, IEEE, 2009.

[11] V. Presada, "Power system state estimator with inclusion of time-synchronized phasor measurements," in *Optimization of Electrical and Electronic Equipment (OPTIM), 2012 13th International Conference on*, pp. 89–94, IEEE, 2012.

[12] M. Shahraeini and M. H. Javidi, "A survey on topological observability of power systems," in *Power Engineering and Automation Conference (PEAM), 2011 IEEE*, vol. 3, pp. 373–376, IEEE, 2011.

[13] N. H. Abbasy and H. M. Ismail, "A unified approach for the optimal pmu location for power system state estimation," *Power Systems, IEEE Transactions on*, vol. 24, no. 2, pp. 806–813, 2009.

[14] J. Chen, P. Shrestha, S.-H. Huang, N. Sarma, J. Adams, D. Obadina, and J. Ballance, "Use of synchronized phasor measurements for dynamic stability monitoring and model validation in ercot," in *Power and Energy Society General Meeting, 2012 IEEE*, pp. 1–7, IEEE, 2012.

[15] V. P. Tran, S. Kamalasadan, and J. Enslin, "Real-time modeling and model validation of synchronous generator using synchrophasor measurements," in *North American Power Symposium (NAPS), 2013*, pp. 1–5, IEEE, 2013.

[16] P. Pourbeik and G. Stefopoulos, "Validation of generic models for stability analysis of two large static var systems in new york using pmu data," in *T&D Conference and Exposition, 2014 IEEE PES*, pp. 1–4, IEEE, 2014.

[17] N. Zhou, Z. Huang, L. Dosiek, D. Trudnowski, and J. W. Pierre, "Electromechanical mode shape estimation based on transfer function identification using pmu measurements," in *Power & Energy Society General Meeting, 2009. PES'09. IEEE*, pp. 1–7, IEEE, 2009.

[18] N. Zhou, Z. Huang, F. Tuffner, J. Pierre, and S. Jin, "Automatic implementation of prony analysis for electromechanical mode identification from phasor measurements," in *Power and Energy Society General Meeting, 2010 IEEE*, pp. 1–8, IEEE, 2010.

[19] J. H. Chow, A. Chakrabortty, M. Arcak, B. Bhargava, and A. Salazar, "Synchronized phasor data based energy function analysis of power transfer paths," in *Power Engineering Society General Meeting, 2006. IEEE*, pp. 5–pp, IEEE, 2006.

[20] J. Quintero, G. Liu, and V. Venkatasubramanian, "An oscillation monitoring system for real-time detection of small-signal instability in large electric power systems," in *Power Engineering Society General Meeting, 2007. IEEE*, pp. 1–8, IEEE, 2007.

[21] A. Chakrabortty, *A Model Reference Approach for Interarea Modal Damping in Large Power Systems*. Springer, 2012.

[22] V. Venkatasubramanian, X. Yue, G. Liu, M. Sherwood, and Q. Zhang, "Wide-area monitoring and control algorithms for large power systems using synchrophasors," in *Power Systems Conference and Exposition, 2009. PSCE'09. IEEE/PES*, pp. 1–5, IEEE, 2009.

[23] F. Hashiesh, H. E. Mostafa, A.-R. Khatib, I. Helal, and M. M. Mansour, "An intelligent wide area synchrophasor based system for predicting and mitigating transient instabilities," *Smart Grid, IEEE Transactions on*, vol. 3, no. 2, pp. 645–652, 2012.

[24] F. R. Gomez, A. D. Rajapakse, U. D. Annakkage, and I. T. Fernando, "Support vector machine-based algorithm for post-fault transient stability status prediction using synchronized measurements," *Power Systems, IEEE Transactions on*, vol. 26, no. 3, pp. 1474–1483, 2011.

[25] J. Yan, C.-C. Liu, and U. Vaidya, "Pmu-based monitoring of rotor angle dynamics," *Power Systems, IEEE Transactions on*, vol. 26, no. 4, pp. 2125–2133, 2011.

[26] P. Kundur, J. Paserba, V. Ajjarapu, G. Andersson, A. Bose, C. Canizares, N. Hatziargyriou, D. Hill, A. Stankovic, C. Taylor, *et al.*, "Definition and classification of power system stability ieee/cigre joint task force on stability terms and definitions," *Power Systems, IEEE Transactions on*, vol. 19, no. 3, pp. 1387–1401, 2004.

[27] T. Van Cutsem and C. Vournas, *Voltage stability of electric power systems*, vol. 441. Springer, 1998.

[28] S. Horowitz, A. G. Phadke, and B. Renz, "The future of power transmission," *Power and Energy Magazine, IEEE*, vol. 8, no. 2, pp. 34–40, 2010.

[29] M. Parashar and J. Mo, "Real time dynamics monitoring system (rtdms): phasor applications for the control room," in *System Sciences, 2009. HICSS'09. 42nd Hawaii International Conference on*, pp. 1–11, IEEE, 2009.

[30] S. Thakur and A. Chakrabortty, "Multi-dimensional wide-area visualization of power system dynamics using synchrophasors," in *Power and Energy Society General Meeting (PES), 2013 IEEE*, pp. 1–5, IEEE, 2013.

[31] R. Klump, R. E. Wilson, and K. E. Martin, "Visualizing real-time security threats using hybrid scada/pmu measurement displays," in *System Sciences, 2005. HICSS'05. Proceedings of the 38th Annual Hawaii International Conference on*, pp. 55c–55c, IEEE, 2005.

[32] C. L. Phillips and H. T. Nagle, *Digital control system analysis and design*. Prentice Hall Press, 2007.

[33] A. Chakrabortty and A. Salazar, "Building a dynamic electro-mechanical model for the pacific ac intertie using distributed synchrophasor measurements," *European Transactions on Electrical Power*, vol. 21, no. 4, pp. 1657–1672, 2011.

[34] S. Nabavi and A. Chakrabortty, "Topology identification for dynamic equivalent models of large power system networks," in *American Control Conference (ACC), 2013*, pp. 1138–1143, IEEE, 2013.

[35] D. Karlsson, M. Hemmingsson, and S. Lindahl, "Wide area system monitoring and control-terminology, phenomena, and solution implementation strategies," *Power and Energy Magazine, IEEE*, vol. 2, no. 5, pp. 68–76, 2004.

[36] "Service area map." iCreate Duke Energy. Accessed: 2014-10-27.

[37] K. Craven, "Power systems for beginners." Internal Refererence Manual, 2013.

[38] "Duke Energy Vision for Synchrophasor Technology," tech. rep., Duke Energy, 2010.

[39] A. Chakrabortty, "Power system stability and control." University Course Lecture Notes, 2014.

[40] M. Glavic and T. Van Cutsem, "A short survey of methods for voltage instability detection," in *Power and Energy Society General Meeting, 2011 IEEE*, pp. 1–8, IEEE, 2011.

[41] S. Dasgupta, M. Paramasivam, U. Vaidya, and V. Ajjarapu, "Pmu-based model-free approach for short term voltage stability monitoring," in *Power and Energy Society General Meeting, 2012 IEEE*, pp. 1–8, IEEE, 2012.

[42] S. Corsi and G. N. Taranto, "A real-time voltage instability identification algorithm based on local phasor measurements," *Power Systems, IEEE Transactions on*, vol. 23, no. 3, pp. 1271–1279, 2008.

[43] X. Wang, H. Sun, B. Zhang, W. Wu, and Q. Guo, "Real-time local voltage stability monitoring based on pmu and recursive least square method with variable forgetting factors," in *Innovative Smart Grid Technologies-Asia (ISGT Asia), 2012 IEEE*, pp. 1–5, IEEE, 2012.

[44] K. Vu, M. M. Begovic, D. Novosel, and M. M. Saha, "Use of local measurements to estimate voltage-stability margin," *Power Systems, IEEE Transactions on*, vol. 14, no. 3, pp. 1029–1035, 1999.

[45] K. T. Vu and D. Novosel, "Voltage instability predictor (vip)method and system for performing adaptive control to improve voltage stability in power systems," Apr. 17 2001. US Patent 6,219,591.

[46] D. Julian, R. Schulz, K. Vu, W. Quaintance, N. Bhatt, and D. Novosel, "Quantifying proximity to voltage collapse using the voltage instability predictor (vip)," in *Power Engineering Society Summer Meeting, 2000. IEEE*, vol. 2, pp. 931–936, IEEE, 2000.

[47] I. Smon, G. Verbic, and F. Gubina, "Local voltage-stability index using tellegen's theorem," *Power Systems, IEEE Transactions on*, vol. 21, no. 3, pp. 1267–1275, 2006.

[48] R. F. Nuqui, A. G. Phadke, R. P. Schulz, and N. Bhatt, "Fast on-line voltage security monitoring using synchronized phasor measurements and decision trees," in *Power Engineering Society Winter Meeting, 2001. IEEE*, vol. 3, pp. 1347–1352, IEEE, 2001.

[49] M. Larsson, C. Rehtanz, and J. Bertsch, "Real-time voltage stability assessment of transmission corridors," in *Proceedings of IFAC Power Plants and Power Systems Control Conference, Seoul, Korea*, 2003.

[50] B. Milosevic and M. Begovic, "Voltage-stability protection and control using a wide-area network of phasor measurements," *Power Systems, IEEE Transactions on*, vol. 18, no. 1, pp. 121–127, 2003.

[51] P. Kessel and H. Glavitsch, "Estimating the voltage stability of a power system," *Power Delivery, IEEE Transactions on*, vol. 1, no. 3, pp. 346–354, 1986.

[52] H. Innah, D. Asfani, and T. Hiyama, "Voltage stability assessment based on discrimination principle," in *Universities Power Engineering Conference (AUPEC), 2012 22nd Australasian*, pp. 1–6, IEEE, 2012.

[53] J. A. Momoh, Y. Xia, and G. Boswell, "Voltage stability enhancement using phasor measurement unit (pmu) technology," in *Power Symposium, 2008. NAPS'08. 40th North American*, pp. 1–6, IEEE, 2008.

[54] L. Warland and A. T. Holen, "A voltage instability predictor using local area measurements (vip++)," in *Power Tech Proceedings, 2001 IEEE Porto*, vol. 2, pp. 6–pp, IEEE, 2001.

[55] M. Glavic and T. Van Cutsem, "Investigating state reconstruction from scarce synchronized phasor measurements," in *PowerTech, 2011 IEEE Trondheim*, pp. 1–8, IEEE, 2011.

[56] C. Rehtanz and J. Bertsch, "Wide area measurement and protection system for emergency voltage stability control," in *Power Engineering Society Winter Meeting, 2002. IEEE*, vol. 2, pp. 842–847, IEEE, 2002.

[57] M. Glavic and T. Van Cutsem, "Wide-area detection of voltage instability from synchronized phasor measurements. part i: Principle," *Power Systems, IEEE Transactions on*, vol. 24, no. 3, pp. 1408–1416, 2009.

[58] D. Q. Zhou, U. Annakkage, and A. D. Rajapakse, "Online monitoring of voltage stability margin using an artificial neural network," *Power Systems, IEEE Transactions on*, vol. 25, no. 3, pp. 1566–1574, 2010.

[59] M. Aldeen, S. Saha, and T. Alpcan, "Voltage stability margins and risk assessment in smart power grids," 2014.

[60] C. Rehtanz and J. Bertsch, "A new wide area protection system," in *Power Tech Proceedings, 2001 IEEE Porto*, vol. 4, pp. 6–pp, IEEE, 2001.

[61] S. Dasgupta, M. Paramasivam, U. Vaidya, and V. Ajjarapu, "Real-time monitoring of short-term voltage stability using pmu data," 2013.

[62] R. Diao, K. Sun, V. Vittal, R. J. O'Keefe, M. R. Richardson, N. Bhatt, D. Stradford, and S. K. Sarawgi, "Decision tree-based online voltage security assessment using pmu measurements," *Power Systems, IEEE Transactions on*, vol. 24, no. 2, pp. 832–839, 2009.

[63] C.-W. Liu, J. S. Thorp, J. Lu, R. J. Thomas, and H.-D. Chiang, "Detection of transiently chaotic swings in power systems using real-time phasor measurements," *Power Systems, IEEE Transactions on*, vol. 9, no. 3, pp. 1285–1292, 1994.

[64] A. Wolf, J. B. Swift, H. L. Swinney, and J. A. Vastano, "Determining lyapunov exponents from a time series," *Physica D: Nonlinear Phenomena*, vol. 16, no. 3, pp. 285–317, 1985.

[65] "Lyapunov exponent: Lecture 24 indian institute of technology kharagpur." YouTube video https://www.youtube.com/watch?v=-xSNqJQRoo4. Accessed: 2014-10-10.

[66] B. de Ville, "Decision trees for business intelligence and dubinske analize-using sas enterprise miner," *SAS Institute, Cary, NC, USA*, 2006.

[67] *SAS Enterprise Miner and SAS Text Miner Procedures Reference for SAS 9.4.*

APPENDIX

Appendix A

Lyapunov Exponent Matrix

This appendix includes the results of the Lyapunov Exponent Matrix covered in chapter four. There are 40 scenarios that cover four load levels, two contingencies and five operating conditions described below.

Load Scenarios:

1. x MW (x = base load)
2. x+400 MW
3. x+1600 MW
4. x+2000 MW

Contingencies:

1. Line Loss (500 kV)
2. Generation Loss (1200 MW)

Table A.1: Operating Conditions

OC Number	Local Generation Support	SVC	Capacitor Bank	Code
1	OFF (g)	OFF (s)	OFF (c)	gsc
2	OFF (g)	OFF (s)	ON (C)	gsC
3	OFF (g)	ON (S)	OFF (c)	gSc
4	OFF (g)	ON (S)	ON (C)	gSC
5	ON (G)	OFF (s)	OFF (c)	Gsc

Figures A.1 and A.2 include the 20 scenarios for the generator loss event and Figures A.3 and A.4 include the 20 scenarios for the line loss event. The first and third columns show the LE spectrum over five minutes. Columns two and five have the time of the final sign change, stability detection time, and the final margin. The five different operating conditions are specified in columns three and six.

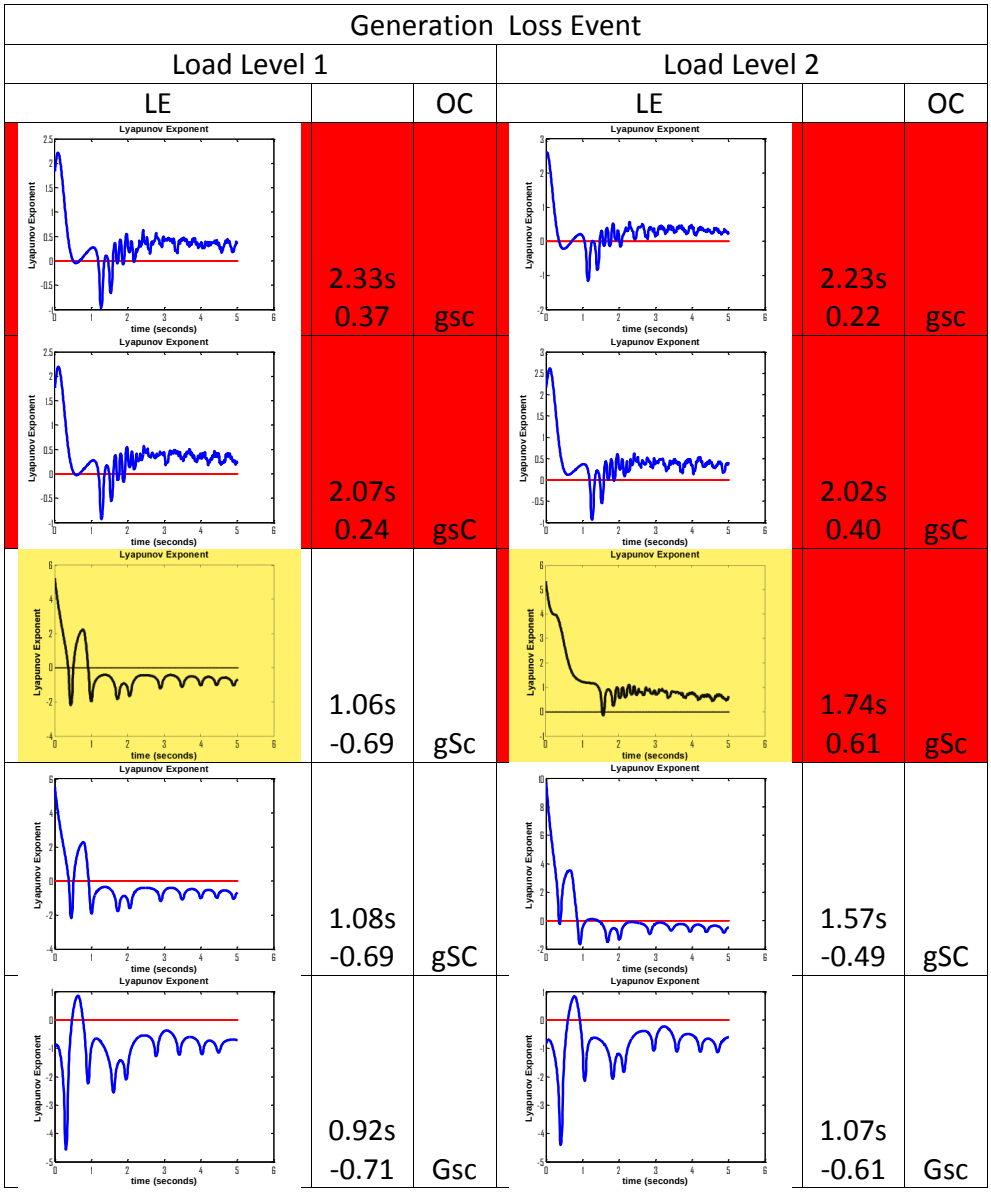

Figure A.1: LE Generator Loss Event Load Scenario 1 and 2

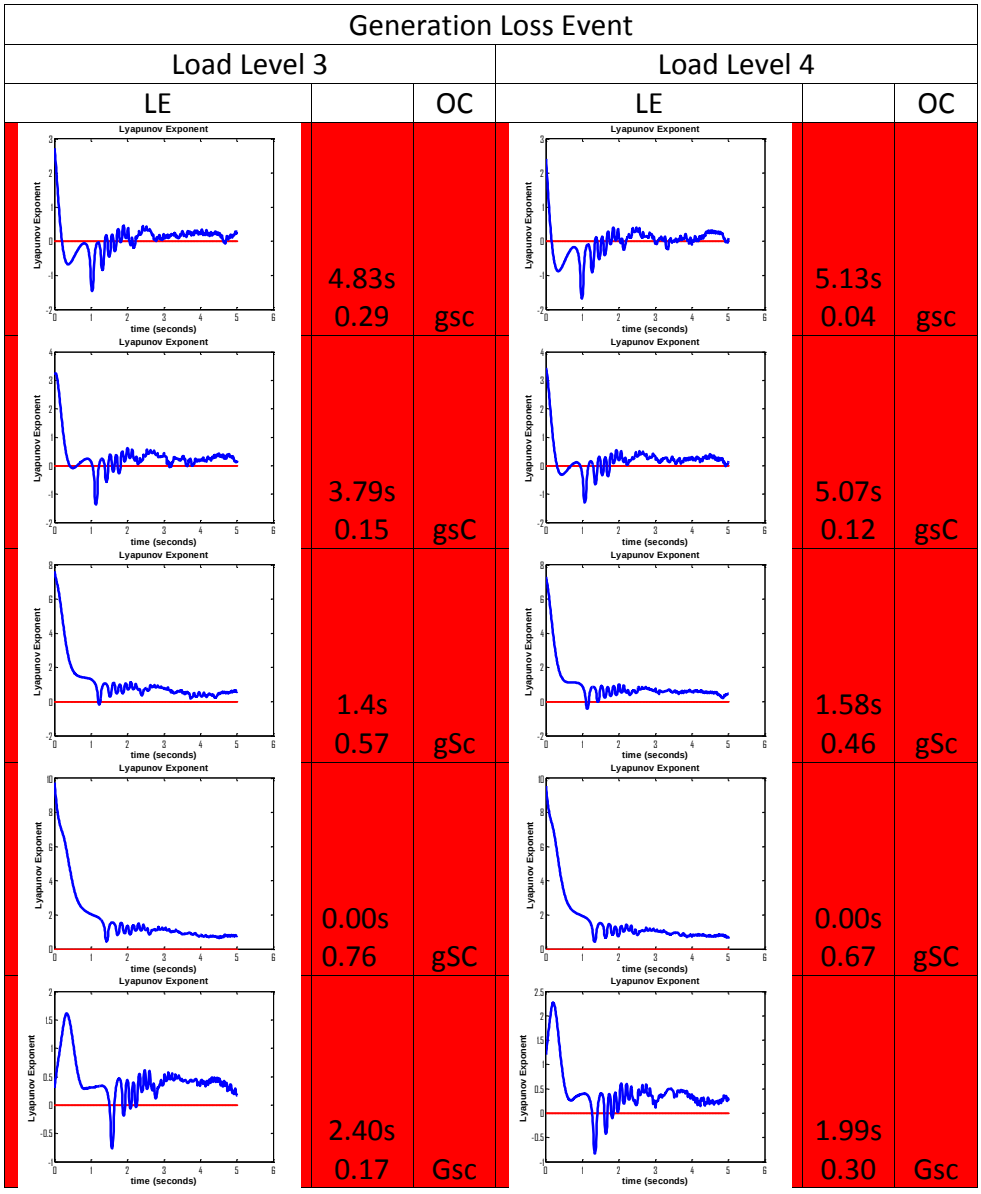

Figure A.2: LE Generator Loss Event Load Scenario 3 and 4

Line Loss Event					
Load Level 1			Load Level 2		
LE		OC	LE		OC
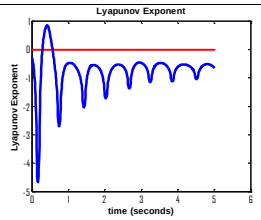	0.71s -0.64	gsc	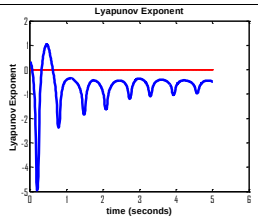	0.77s -0.49	gsc
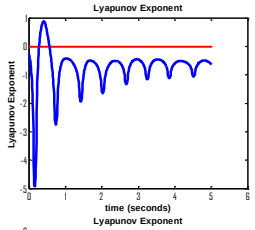	0.71s -0.63	gsC	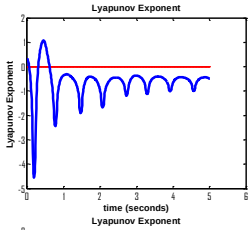	0.76s -0.49	gsC
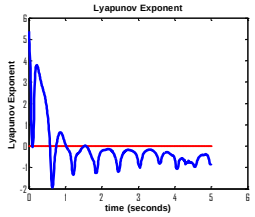	1.72s -0.85	gSc	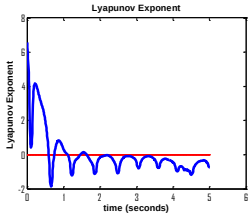	1.78s -0.73	gSc
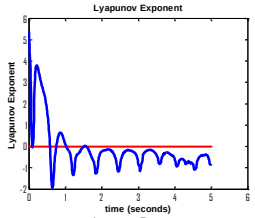	1.72s -0.84	gSC	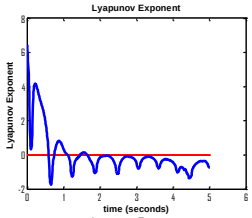	1.79s -0.74	gSC
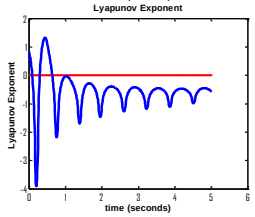	0.78s -0.57	Gsc	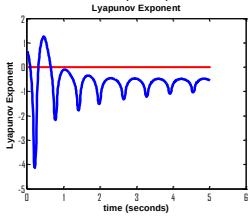	0.79s -0.54	Gsc

Figure A.3: LE Line Loss Event Load Scenario 1 and 2

Line Loss Event					
Load Level 3			Load Level 4		
LE		OC	LE		OC
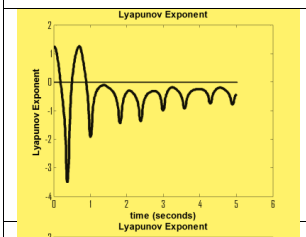	1.03s -0.43	gsc	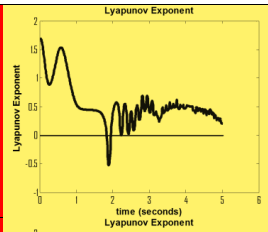	2.09s 0.21	gsc
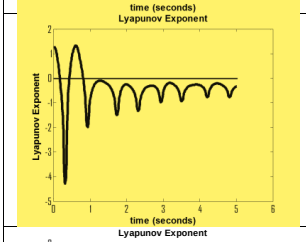	0.95s -0.34	gsC	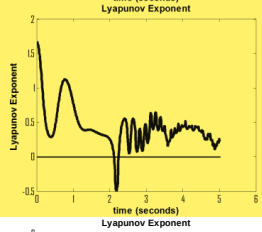	2.38s 0.26	gsC
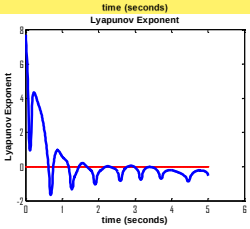	3.11s -0.47	gSc	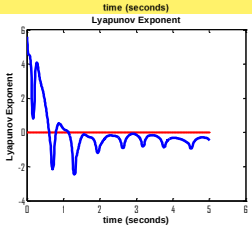	1.28s -0.44	gSc
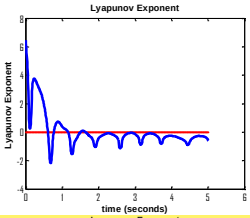	1.78s -0.58	gSC	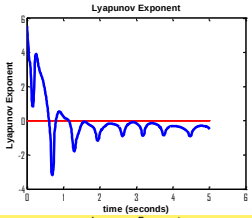	1.29s -0.46	gSC
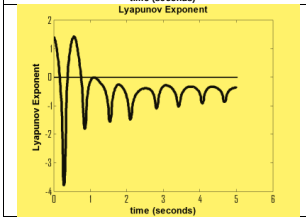	0.90s -0.38	Gsc	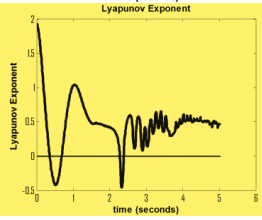	2.52s 0.47	Gsc

Figure A.4: LE Line Loss Event Load Scenario 3 and 4